8

DS

The San Andreas Fault in Southern California

from Carrizo Plain to Cajon Pass

A Study of Recurrence Intervals, Slip Rates and Geomorphic Features

A CSUN Interim Field Trip

by

H. Adams and G. Simila

January 23 and 24, 1987

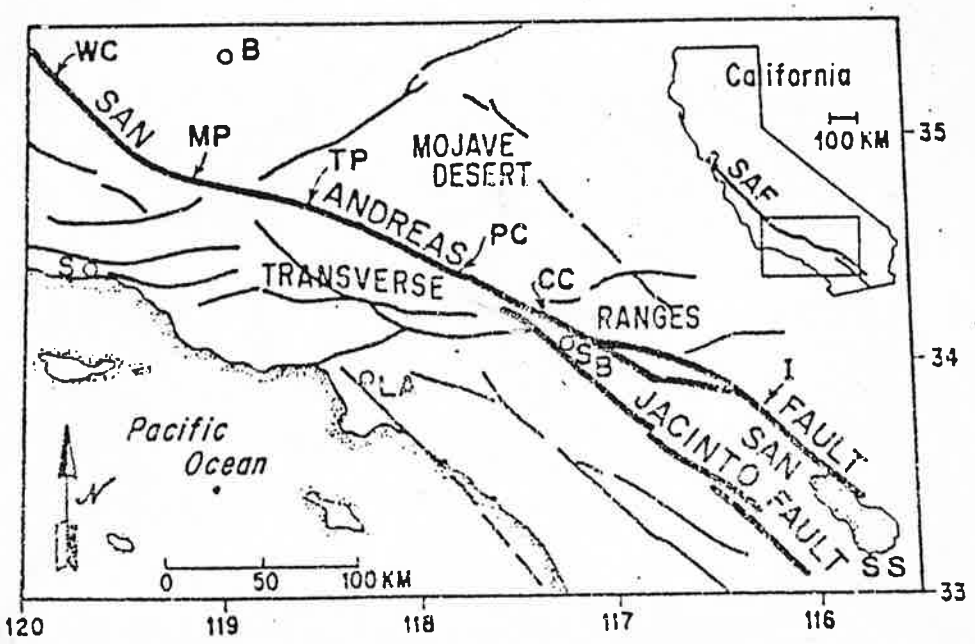

WARNING: This field trip may be hazardous to your health. The San Andreas Fault is subject to violent shaking and displacement at any moment and may result in severe psychic trauma, whiplash, or even burial by the resulting chasms. Attend at your own risk and remember - its not our fault!

Introduction

After the 1906 San Francisco earthquake, Reid in 1911 proposed his now accepted theory of the elastic rebound theory. In addition, he introduced the concept of the recurrence interval based on observations of survey data points in the San Francisco Bay region and offset along the San Andreas fault during the 1906 event. The concept of the recurrence interval was later modified by Robert Wallace in his paper in 1970 and to the form

$$R = D/(S-C)$$

where "R" is the recurrence interval or return period of the earthquake in years, "D" is the displacement in meters during any given earthquake event, "S" is the long-term geologic slip rate, and "C" is the creep rate.

Recent attempts in seismic hazard evaluation have focused on this relationship where the seismic risk is a function of the probability of an earthquake of a given magnitude recurring. (It can be shown that the magnitude of an earthquake event is proportional to the displacement D that takes place on the fault during any given earthquake event.) We will visit areas where studies have focused on these fault characteristics.

Our field trip will take us along the San Andreas Fault, where we will observe many recent geomorphic features along the fault, and features associated with particular earthquake events. In addition to the geomorphic features along the fault, we will visit several classic localities where recent detailed geologic studies have been undertaken. Detailed mapping of sections of the fault, and detailed subsurface investigation by trenching along and across the fault combined with radiocarbon dating of these very recent sediments have enabled geologists to determine recurrences of individual earthquake events, long term geologic slip rates, and displacements of individual earthquake events. The primary goal in determining geologic slip rates, is to determine the age and amount of offset of piercing points which cross the fault. These piercing points are geologic linear features, such as angular unconformities, axes of anticlines or synclines, terrace risers, and particularly stream channels.

Our first day's field trip will focus on the north end of the southern section of the San Andreas fault, which begins just south of Cholame in the Carrizo plain where due to the semi-arid nature of the Carrizo plain area, most of the recent geomorphic features are incredibly well preserved (see Wallace's article attached). Features as old as thirteen thousand years old which have been dated by radiocarbon dates can still be recognized, and are still being used to determine long term geologic slip rates for this section of the fault. Our first locality that we will visit will be Wallace Creek (see excerpts from Sieh and Jahn's article attached), where detailed studies have determined both a long term geologic slip rate and offsets of individual earthquakes which have offset stream channels which cross the fault.

The remainder of the day will be spent visiting additional geomorphic features along the San Andreas fault (see attached block diagram).

Day two will focus on the section of the San Andreas fault from Palmdale to Cajon Pass. Stops will include the Palmdale Reservoir overlook, Una Lake and then along the fault to Emma Road fanglomerate east of the mouth of Little Rock Creek. We will then visit a site along the fault that is currently being trenched and logged by the USGS (Schwartz and Weldon). Then on to Pallett Creek (see excerpts from articles by Kerry Sieh) where earthquake recurrence intervals have been determined directly by fault features and radiocarbon dating.

Lunch stop at the Mormon Rocks in Cajon Pass and then a visit to the DOSECC drill site in Cajon Pass. The last two stops will be in Cajon Pass where we will look at the effects the San Andreas fault has had on stream terraces and stream channels.(See excerpts from the Weldon article attached).

(An optional last stop for the fault hardy will be to observe the 30+ meter vertical offset of the Cucamonga fault where it crosses the Day Canyon alluvial fan).

From: CDMG SR 118, 1975

THE SAN ANDREAS FAULT IN THE CARRIZO PLAIN-TEMBLOR RANGE REGION, CALIFORNIA

By Robert E. Wallace
U.S. Geological Survey
Menlo Park, California 94025

ABSTRACT

Geomorphic features characteristic of the San Andreas fault zone are exceptionally well displayed in the Carrizo Plain-Temblor Range region, California. Offset stream channels, elongate grabens, sags, and linear ridges are among the fault-related features found in the area. As a result of movement on the San Andreas fault during the earthquake of 1857, many stream channels were offset, some by as much as 10-11 m. One estimate of the recurrence interval between earthquakes as large as that of 1857 is about 700 years.

INTRODUCTION

Many geomorphic features associated with the San Andreas fault are classically displayed along a segment of the fault from about 100 to 200 km (60-120 mi) northwest of Los Angeles. There, between the Temblor and Caliente Ranges, the fault passes through an arid region in which most landforms are unobscured by vegetation.

Bordering the fault on the southeast is an area of low relief known as the Carrizo Plain. Soda Lake, an ephemeral, saline lake, lies in a low, undrained part of the plain. To the northeast are a series of hills, including the Elkhorn and Panorama Hills, that might be considered the western flank or foothills of the Temblor Range.

The boundary between the hills and plains broadly marks the trace of the San Andreas fault zone, but the most striking geomorphic expressions of individual fault strands generally are linear troughs, valleys, gulches, and scarplets, just within the southwest flanks of the hills, or crossing parts of the Carrizo Plain near or between the hills. Many of the valleys and gulches are erosional features, formed by the action of intermittent streams that flow from the Temblor Range to the fault where they are deflected and cut channels in the more easily eroded brecciated and disturbed rocks along the fault. Some patterns of channels are more a result of right-lateral slip along the fault than of differential erosion alone. Among the characteristics and patterns formed by these processes are offset or beheaded channels, "Z"-shaped channels, deflected drainage and trellis drainage, warped or curved drainage, and en echelon channels (see Fig. 2).

Many geomorphic features result chiefly from differential uplift or depression, block tilting or warping, or lateral differential movement. Among these features of primarily tectonic origin are elongate grabens or troughs, sag ponds, linear scarplets and ridges, tilted and rotated blocks, shutter ridges, medial ridges, en echelon lineaments, and fold ridges.

ROCKS ALONG THE FAULT

The San Andreas fault divides the region into very dissimilar blocks of basement rocks and overlying sedimentary sequences (Dibblee, 1973a; Addicott, 1968). Large-scale (tens or hundreds of kilometres) strike slip in a right-lateral sense has juxtaposed these dissimilar blocks. Some of the evidence and arguments for this large slip are reviewed by J. G. Vedder in a companion paper in this volume.

The dominant rock units exposed at the surface, within a kilometre or so of the fault trace, are relatively young geologically, including Pliocene, Pleistocene, and Holocene sediments (see Vedder, 1970; Dibblee, 1973a, 1973b).

Most of these deposits are nonmarine gravel, sand, and silt derived locally from the Temblor Range. They are poorly to moderately indurated. At a few places rocks as old as Miocene are exposed near the fault.

The Morales Formation, of Pliocene age, and Paso Robles Formation, of Pliocene(?) and Pleistocene age, are extensively exposed in the Panorama Hills. In the Elkhorn Hills the Paso Robles Formation forms more than 90 percent of the outcrops. Alluvium and terrace deposits of several ages can be recognized, as well as numerous landslide deposits.

OFFSET AND DEFLECTED STREAMS

One of the most convincing lines of evidence for right-lateral strike slip on the San Andreas fault is that based on offset stream channels. These are nowhere better displayed than in the Carrizo Plain area. Arnold and Johnson (1910), Willis (1925), and Wood and Buwalda (1931) described some of these features. Wallace (1968) found more than 130 channels between Cholame and Camp Dix that appeared to display true offset by right-lateral slip, a few by more than 1,000 m.

Many channels are offset by 7 to 14 m a particularly common offset is between 10 and 11 m (see Wallace, 1968). Some of the small channels offset by 10-11 m appear to have been displaced by a single episode of movement and thus may represent displacement related to the 1857 earthquake. Figure 1, for example, shows two small channels that slope toward the viewer. The trace of the San Andreas fault bisects the frame from left to right. The channel at the left is beheaded at the fault trace at the uphill edge of the clump of vegetation in the channel. Presumably the uphill segment of the channel at the right was originally the headwaters of the channel at the left. The microgeomorphology between the two channels suggests no period of intermediate offset during which intermediate channels or bends of channels were carved. Rather, the terrain suggests one sudden offset of between 10 and 11 m. This set of channels is one of several good examples of offset channels in sec. 11, T. 32 S.,

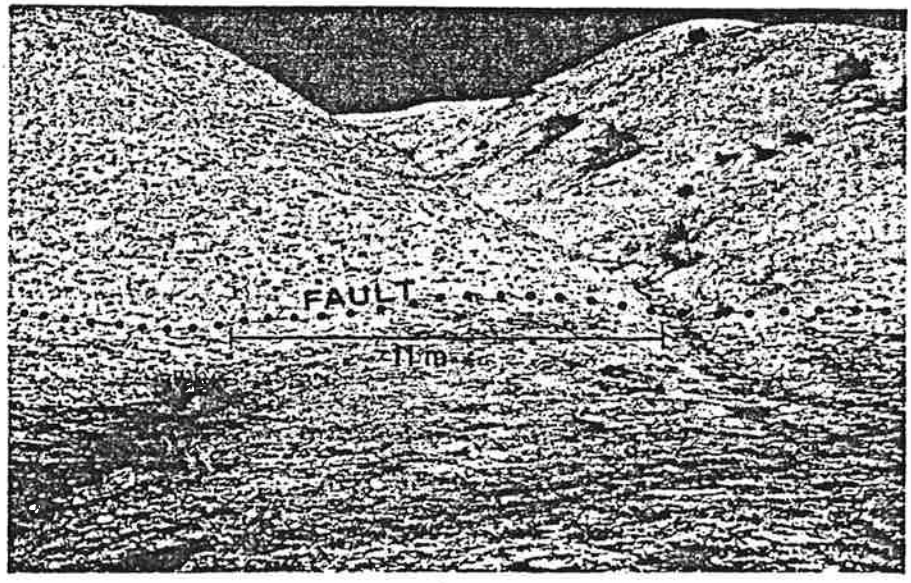

Figure 1. Channel at left (note dark vegetation) may have been displaced in 1857 about 11 m from the channel at right.

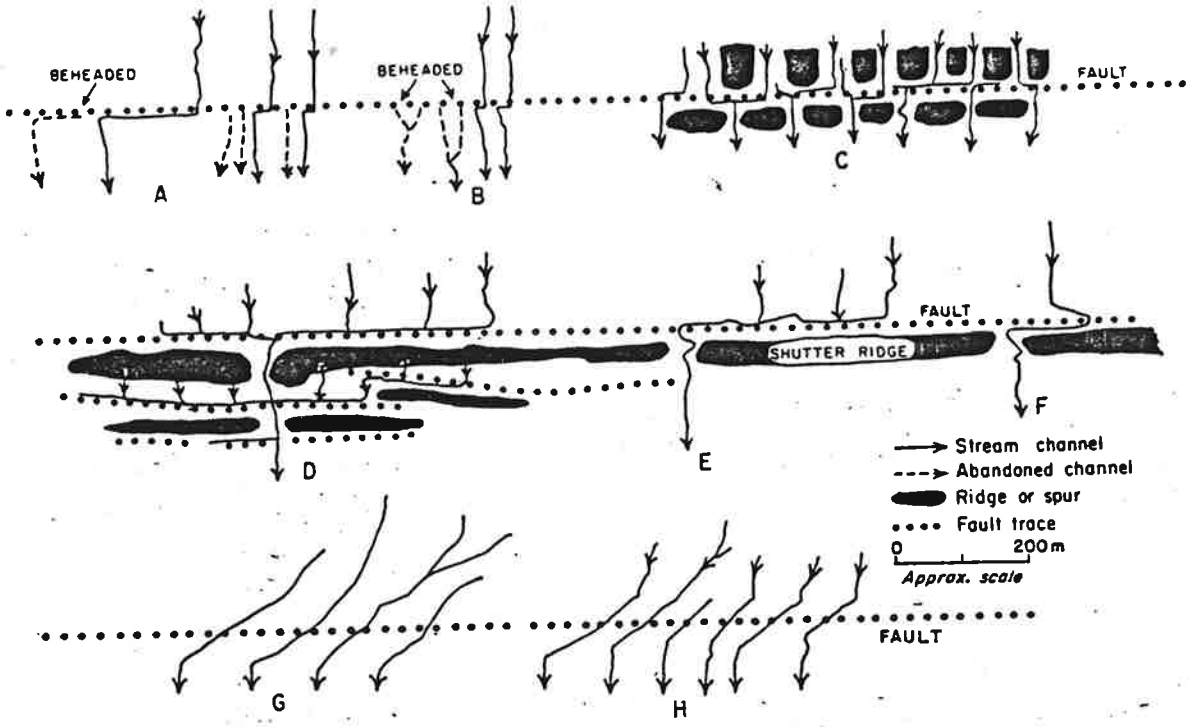

Figure 2. Diagrammatic representation of patterns of fault-related stream channels found in the Carrizo Plain area.

OFFSET CHANNELS

A. Misalinement of single channels directly related to amount of fault displacement and age of channel. No ridge on downslope side fault. Beheading common.
B. Paired stream channels misalined.

COMBINATION OF OFFSET AND DEFLECTION

C. Compound offsets of ridge spurs, and offset and deflection of channels. Both right and left deflection.
D. Trellis drainage produced by multiple fault strands, sliver ridges, and shutter ridges.
E. Offset plus deflection by shutter ridge may produce exaggerated or reversed apparent offset.
F. Capture by adjacent channel followed by right-lateral slip may produce "Z" pattern.

FALSE OFFSETS

G. Differential uplift may deflect streams to produce false offset.
H. En echelon fractures over fault zone followed by subsequent streams produce false offset.

R. 21 E., in the Panorama Hills quadrangle. Each offset or deflected channel system presents a different microgeomorphologic problem, no two of which are identical. Wallace (1968, p. 10) noted that stream channels of small or intermediate size (100-500 m long) best record displacements of a few metres, whereas longer stream channels best record larger displacements.

The factor that probably complicates the drainage patterns most drastically and makes interpretation difficult is vertical tectonic movement. Uplift of only a few centimetres of the block under the downslope segment of a stream may be enough to deflect a small stream, and if a linear block along the fault is raised by as much as several metres across the general drainage pattern, large deflections, both right or left lateral, can result. Figure 2 diagrammatically illustrates some characteristic situations; most are represented in the Carrizo Plain area.

Some left-lateral channel offsets are recorded that are as yet unexplained by deflection, and it should be kept in mind that local left-lateral slip is possible within an overall right-lateral strain field. For example, a thrust or differentially folded block might be bounded by left-lateral slip on one side and right-lateral slip on the other.

VERTICAL DISPLACEMENTS

Inasmuch as the San Andreas fault is characterized by tens, and possibly even hundreds, of kilometres of strike slip, it should not seem surprising that local blocks a few kilometres or less on a side are jostled differentially along the fault and move either up or down by as much as a kilometre or more during the active life of the fault. The ratio of vertical to horizontal movement may be about 1 to 10 or 1 to 20. On a small scale, for example, scarplets up to a metre or so high seem fresh enough to be related to the 1857 event in which 10 m of right-lateral slip probably occurred. As one walks along the most recently active trace, one can find alternately scarps facing southwest and northeast. Apparently block movement or buckling differentially raised or depressed adjacent areas.

Sags (or "sag ponds" if filled with water) are very common and result where irregularities in the fault trace create local tension and collapse of blocks between branches or strands of the fault Sags generally are a few hundred metres long and a few metres to tens of metres wide. They may lie from a fraction of a metre to several metres below the surrounding terrain. Elongate grabens similarly are depressed blocks between parallel branches of the fault (Fig. 3).

The Elkhorn Hills are an elongate upwarp, the crest of which is broken into a series of grabens. Some of the grabens have a sigmoid pattern (see Fig. 4), suggestive of broad strike-slip strain. The upwarp may have formed when gouge and brecciated material in a fault zone approximately 2 km wide was squeezed upward in a semi-plastic state by regional stresses normal to the fault zone. The overlying, poorly consolidated, Paso Robles Formation, once upraised, has slid laterally, producing large areas of landslides on the flanks of the upwarp and grabens at the crest. The grabens were later bowed by right-lateral strain into the sigmoid patterns now present. Large landslide blocks moved southwest, crossed the most active strand of the San Andreas fault, and were then transported northwestward from their original position. The elongate block "A" (Fig. 4) may be such a transported landslide block.

SEISMICITY AND FAULT MOVEMENT

This segment of the San Andreas fault is seismically very quiet at present (Brune and Allen, 1967), although the great earthquake of 1857 probably had a magnitude greater than 8. Fault offset

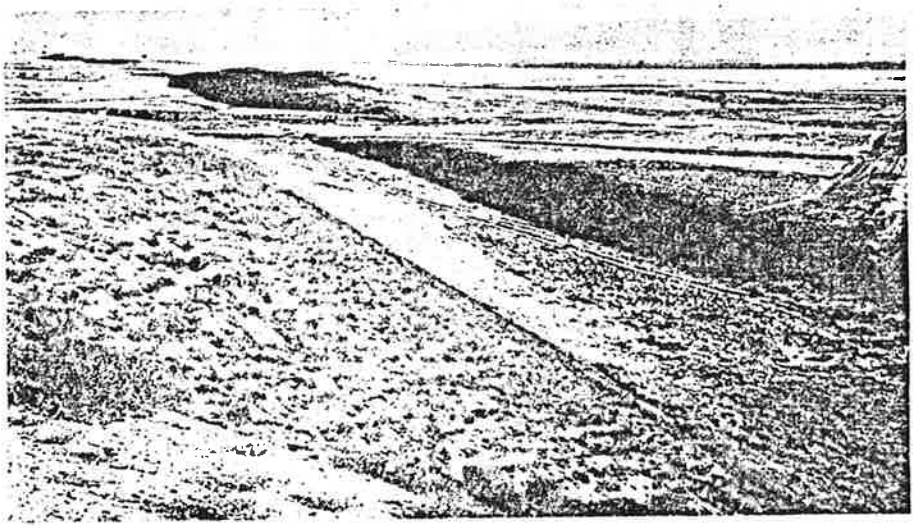

Figure 3. Elongate graben along San Andreas fault.

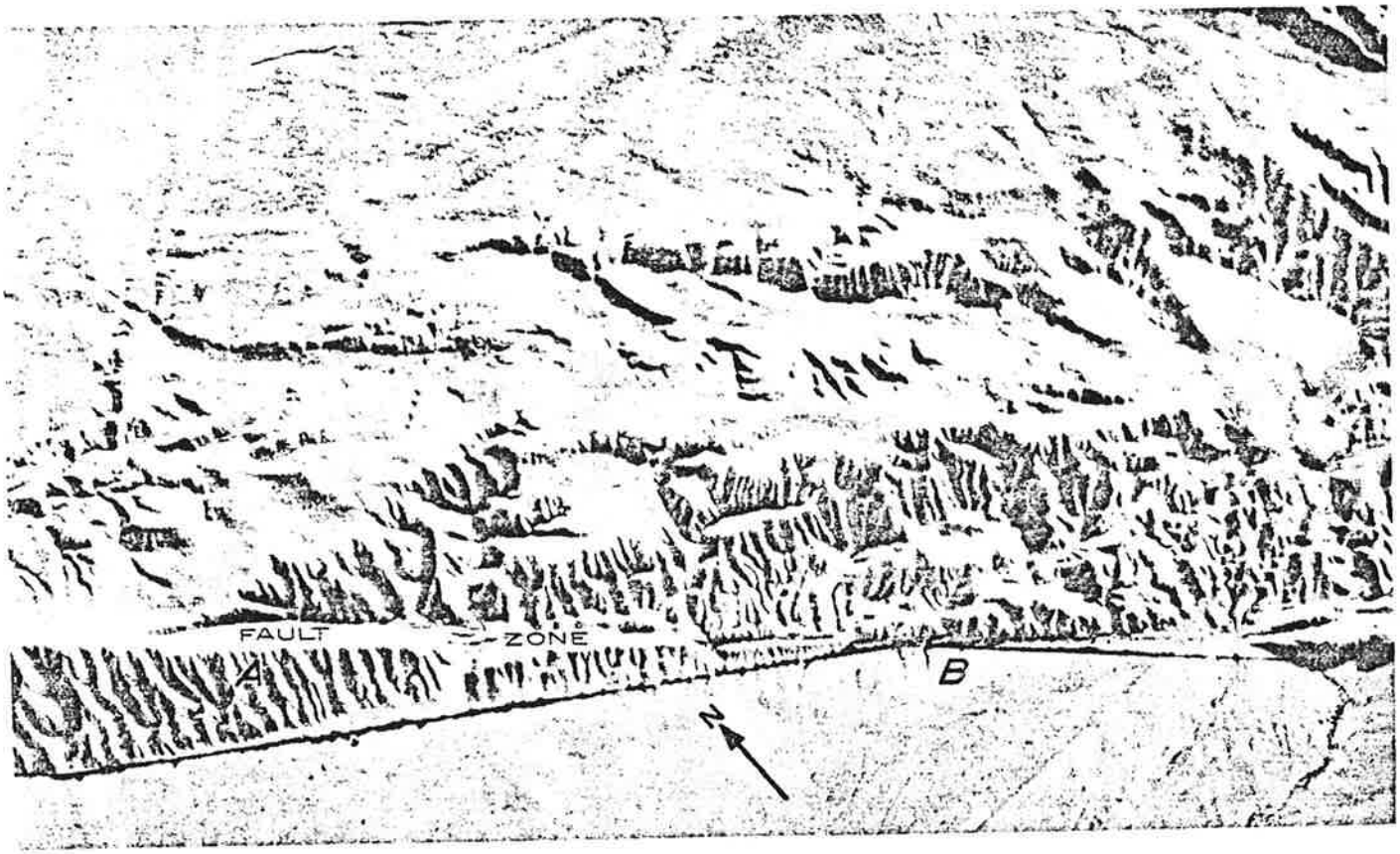

Figure 4. Grabens at crest of Elkhorn Hills. Note sigmoid pattern of some. Block "A" may be landslide block moved laterally from "B."

during the 1857 earthquake was not accurately recorded, but a circular corral, described by Wood (1955), was offset to produce an "S" shape and clearly demonstrated right-lateral slip of several metres. Numerous small stream channels display offsets of from 7 to 15 m (Wallace, 1968) and warrant the assumption that fault displacements in this range probably occurred in 1857.

Geodimeter measurements made during the period 1959 to 1973 (Savage and others, 1973) indicate very small strain rates. One geodimeter line, trending north-south about 30 km and crossing the fault due west of Taft, shows no appreciable change in length between 1959 and 1973. Examination of fences up to 50 years old that cross the fault revealed no measurable misalinement (Brown and Wallace, 1968).

The amount of displacement of distinctive geologic units suggests offset rates in the range of 1.4 to 2.1 cm per year for the past 10 to 20 million years (Clarke and Nilsen, 1973; Grantz and Dickinson, 1968). The contrast between the long-term rate and the slow or negligible movement in the past few decades has led some workers to describe this segment of the fault as being locked. "Locked," in this sense, conveys the interpretation that elastic strain continues to build up uniformly at a rate equivalent to the long-term offset rate, but that for some reason this segment of the fault is unable to slip and accommodate the elastic strain at present. Rupture can be expected at some time in the future when the strength of the lock is exceeded.

Tectonic slip or "creep," although unknown in this segment of the fault, characterizes the segment to the northwest from Cholame to San Juan Bautista. There, in a few places, measured creep rates very nearly match the long-term offset rate of geologic units, although over much of the segment creep rates are less than 1 cm per year.

EARTHQUAKE RECURRENCE

Repeatedly the question arises, "How often will a great earthquake occur?" One approach to an answer for this segment of the fault is to compare the approximately 10 m of offset that possibly accompanied the 1857 earthquake with the long-term geologic rate of movement of approximately 2 cm per year. At a constant rate of 2 cm per year of elastic strain buildup, 500 years would elapse before the potential for 10 m offset was accumulated. At the rate of 1.4 cm per year, approximately 700 years of accumulation would be required.

Another approach is based on counting small earthquakes that occur often enough for statistical comparisons of numbers of earthquakes at several magnitudes. On a logarithmic graph, the magnitude-census relation plots approximately as a straight line, the slope is expressed as a "b" value, and extrapolation to large infrequent earthquakes is believed to give a useful evaluation of recurrence. An estimate by Allen and others (1965) of the interval between magnitude 8 shocks on the San Andreas fault in southern California based on this approach is 18,300 years, which they concede seems "grossly misleading."

These statements of recurrence interval (sometimes referred to as return period) do not imply that one magnitude 8 earthquake can be expected regularly every 700 years, but rather that over geologic time this would be the average. A better way to state this relation is that there is a 1-in-700 chance (or .14 percent chance) of a great earthquake each year. Even this grossly oversimplifies the problem because it assumes a statistical homogeneity and ignores the likelihood of clustering of events in time. Clustering of major events may be more common than we can now tell from the short recorded history of the fault, so that several major earthquakes may occur within a century, separated by a thousand years or more of no large

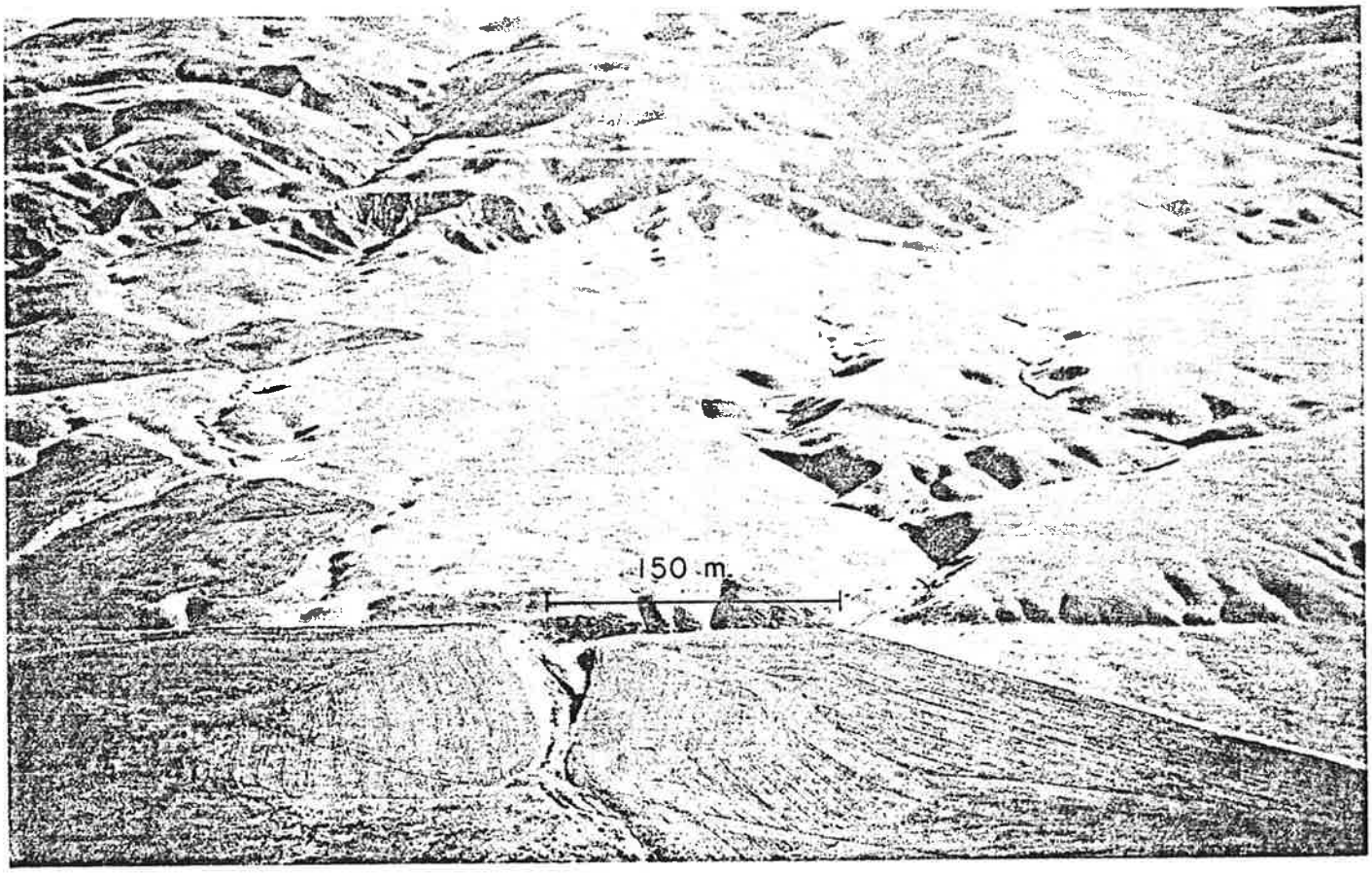

Figure 5. Stream channel offset about 150 m. Temblor Range in background.

Figure 6. Pattern of channels appears to be controlled by en echelon fractures over the San Andreas fault zone. Note that these are right-stepping, comparable to thrust shears (see Wallace, 1973).

events. In the Caliente Range, Clifton (1968) found sedimentary cycles suggesting tectonic "events (or closely spaced flurries of events) with a periodicity of tens of thousands of years" which he relates to possible recurrent movement along the San Andreas fault.

WHERE TO SEE FAULT FEATURES

A field trip to see excellent features of the fault can be taken on secondary roads between State Highway 58 near Simmler and Highway 33 west of Maricopa. For a field guide map in this area, see the map by Vedder and Wallace (1970).

Starting at State Highway 58 (formerly 178) near Simmler (between Bakersfield and San Luis Obispo), one can take a dirt road in sec. 17, T. 31 S., R. 2 E., southeast from sec. 17, T. 31 S., R. 2 E. The road runs within a few metres of the fault marked by a northeast-facing scarp. In secs. 33 and 34 is one of the clearest examples of stream channel offset (see Fig. 5). Nearby in sec. 3, T. 31 S., R. 20 E., are excellent examples of sags and sag ponds. This is one of the longest (about 14 km) and straightest fault strands of the entire San Andreas fault system. Displacement, as indicated by offset streams, appears to die out to the southeast on this fault strand to be taken up on the next strand to the southeast.

In secs. 29 and 33, T. 31 S., R. 21 E., an elongate graben is well displayed. In its northwestern half, small fault-bounded blocks lie between the two bounding faults and appear in aerial photographs almost as "roller bearings" between the two blocks. In the NW¼ of sec. 11, T. 32 S., R. 21 E., is an excellent set of offset channels, one of which is shown in Figure 1 and may have been offset in 1857.

Along the Elkhorn scarp in secs. 29 and 33, T. 32 S., R. 22 E., an elongate ridge, essentially a shutter ridge, diverts the major drainage from the Temblor Range. Numerous narrow benches and fresh-appearing scarplets in this area may reflect 1857 movement. Sigmoid grabens are to be found in sec. 34, T. 32 S., R. 22 E., northeast of the Elkhorn scarp (see Fig. 4).

A complex zone of modified en echelon fractures, rather than a continuous, linear fracture, marks the main trace of the fault in sec. 22, T. 11 N., R. 25 W. (see Fig. 6). Strain may be distributed across the entire 1- to 2-km width of the Elkhorn Hills.

From State Highway 33, for a distance of about 4 km northwest, is a series of well-developed sags and sag ponds. From Highway 33 southeast a good paved road follows the fault for about 5 km, crossing the fault twice before winding and climbing to the southwest. Numerous linear ridges representing slivers of rocks between fault strands are visible here.

ACKNOWLEDGMENTS

Reviewed by R. D. Brown, Jr., and J. G. Vedder.

REFERENCES CITED

Addicott, W. O., 1968, Mid-Tertiary zoogeographic and paleogeographic discontinuities across the San Andreas fault, California: in Dickinson, W. R., and Grantz, Arthur, eds., Proceedings of the conference on geologic problems of San Andreas fault system: Stanford Univ. Pubs. Geol. Sci., v. 11, p. 144-165.

Allen, C. R., St. Amand, P., Richter, C. F., and Nordquist, J. M., 1965, Relationship between seismicity and geologic structure in the southern California region: Seismol. Soc. America Bull., v. 55, n. 4, p. 753-797.

Arnold, Ralph, and Johnson, H. R., 1910, Preliminary report on the McKittrick-Sunset oil region, Kern and San Luis Obispo Counties, California: U.S. Geol. Survey Bull. 406, p. 101-102.

Brown, R. D., and Wallace, R. E., 1968, Current and historic fault movement along the San Andreas fault between Paicines and Camp Dix, California: in Dickinson, W. R., and Grantz, Arthur, eds., Proceedings of the conference on geologic problems of San Andreas fault system: Stanford Univ. Pubs. Geol. Sci., v. 11, p. 22-41.

Brune, J. N., and Allen, C. R., 1967, A micro-earthquake survey of the San Andreas fault system in southern California: Seismol. Soc. America Bull., v. 57, n. 2, p. 277-296.

Clark, S. H., and Nilsen, T. H., 1973, Displacement of Eocene strata and implications for the history of offset along the San Andreas fault, central and northern California: in Kovach, R. L., and Nur, Amos, eds., Proceedings of the conference on tectonic problems of the San Andreas fault system: Stanford Univ. Pubs. Geol. Sci., v. 13, p. 358-367.

Clifton, H. E., 1968, Possible influence of the San Andreas fault on middle and probably late Miocene sedimentation, southeastern Caliente Range: in Dickinson, W. R., and Grantz, Arthur, eds., Proceedings of the conference on geologic problems of San Andreas fault system: Stanford Univ. Pubs. Geol. Sci., v. 11, p. 183-190.

Dibblee, T. W., Jr., 1973a, Stratigraphy of the southern Coast Ranges near the San Andreas fault from Cholame to Maricopa, California: U.S. Geol. Survey Prof. Paper 764, 122 p.

Dibblee, T. W., Jr., 1973b, Regional geologic map of San Andreas and related faults in Carrizo Plain, Temblor, Caliente, and La Panza Ranges and vicinity, California: U.S. Geol. Survey Misc. Geol. Inv. Map I-757, scale 1:125,000.

Grantz, Arthur, and Dickinson, W. R., 1968, Indicated cumulative offsets along the San Andreas fault in the California Coast Ranges: in Dickinson, W. R., and Grantz, Arthur, eds., Proceedings of the conference on geologic problems of San Andreas fault system: Stanford Univ. Pubs. Geol. Sci., v. 11, p. 117-119.

Savage, J. C., Prescott, W. H., and Kinoshita, W. T., 1973, Geodimeter measurements along the San Andreas fault: in Kovach, R. L., and Nur, Amos, eds., Proceedings of the conference on tectonic problems of the San Andreas fault system: Stanford Univ. Pubs. Geol. Sci., v. 13, p. 44-53.

Vedder, J. G., 1970, Geologic map of the Wells Ranch and Elkhorn Hills quadrangles, San Luis Obispo and Kern Counties, California: U.S. Geol. Survey Misc. Geol. Inv. Map I-585, scale 1:24,000.

Vedder, J. G., and Wallace, R. E., 1970, Map showing recently active breaks along the San Andreas and related faults between Cholame Valley and Tejon Pass, California: U.S. Geol. Survey Misc. Geol. Inv. Map I-574, scale 1:24,000.

Wallace, R. E., 1968, Notes on stream channels offset by the San Andreas fault, southern Coast Ranges, California: in Dickinson, W. R., and Grantz, Arthur, eds., Proceedings of the conference on geologic problems of San Andreas fault system: Stanford Univ. Pubs. Geol. Sci., v. 11, p. 144-165.

Wallace, R. E., 1973, Surface fracture patterns along the San Andreas fault: in Dickinson, W. R., and Grantz, Arthur, eds., Proceedings of the conference on geologic problems of San Andreas fault system: Stanford Univ. Pubs. Geol. Sci., v. 11, p. 248–250.

Willis, Robin, 1925, Topography of active faulting in California (abs.): Geol. Soc. America Bull., v. 36, n. 1, p. 143–144.

Wood, H. O., 1955, The 1857 earthquake in California: Seismol. Soc. America Bull., v. 45, n. 1, p. 47–67.

Wood, H. O., and Buwalda, J. P., 1931, Horizontal displacement along the San Andreas fault in the Carrizo Plain, California (abs.): Geol. Soc. America Bull., v. 42, n. 1, p. 298–299.

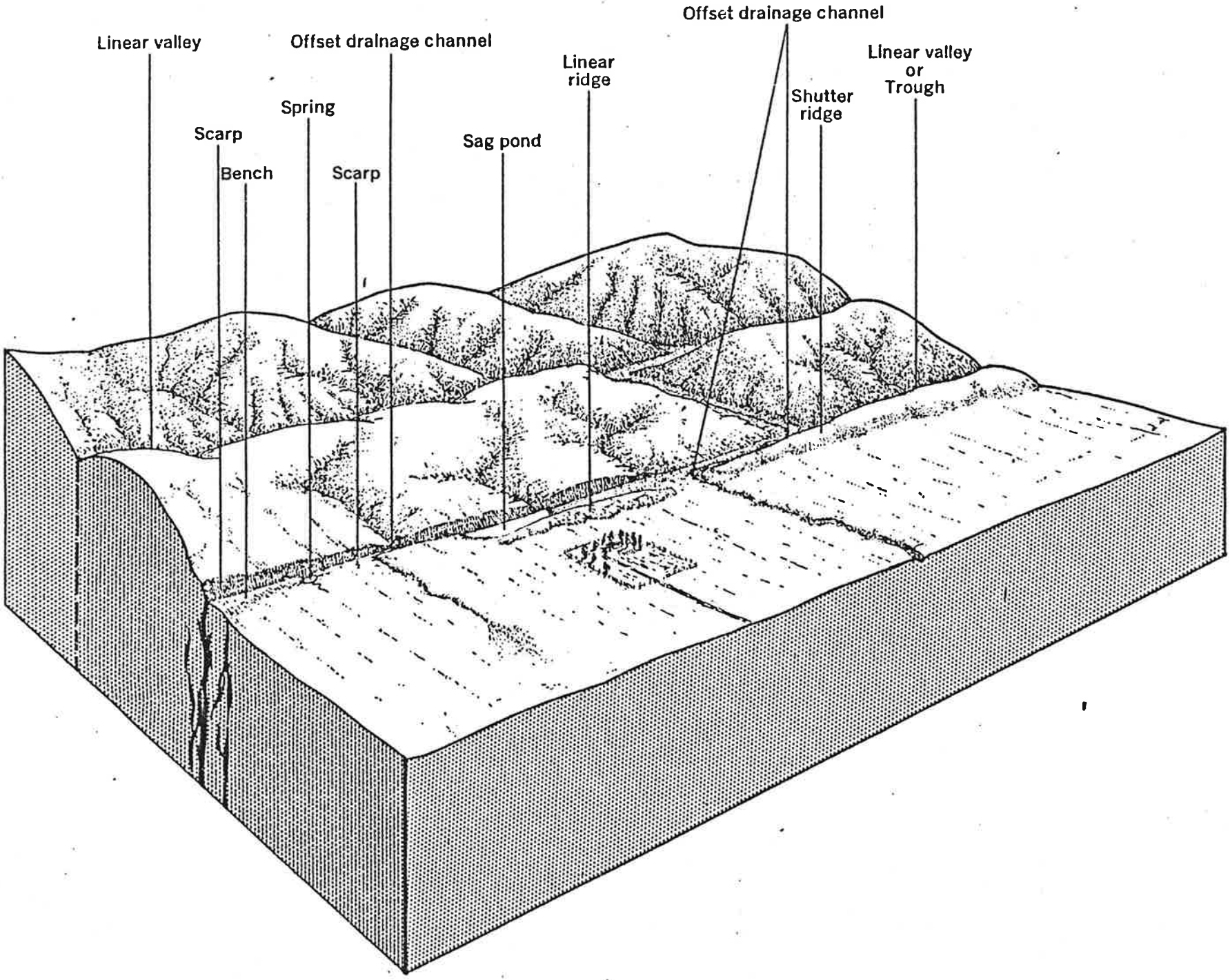

BLOCK DIAGRAM SHOWING LANDFORMS PRODUCED ALONG RECENTLY ACTIVE FAULTS

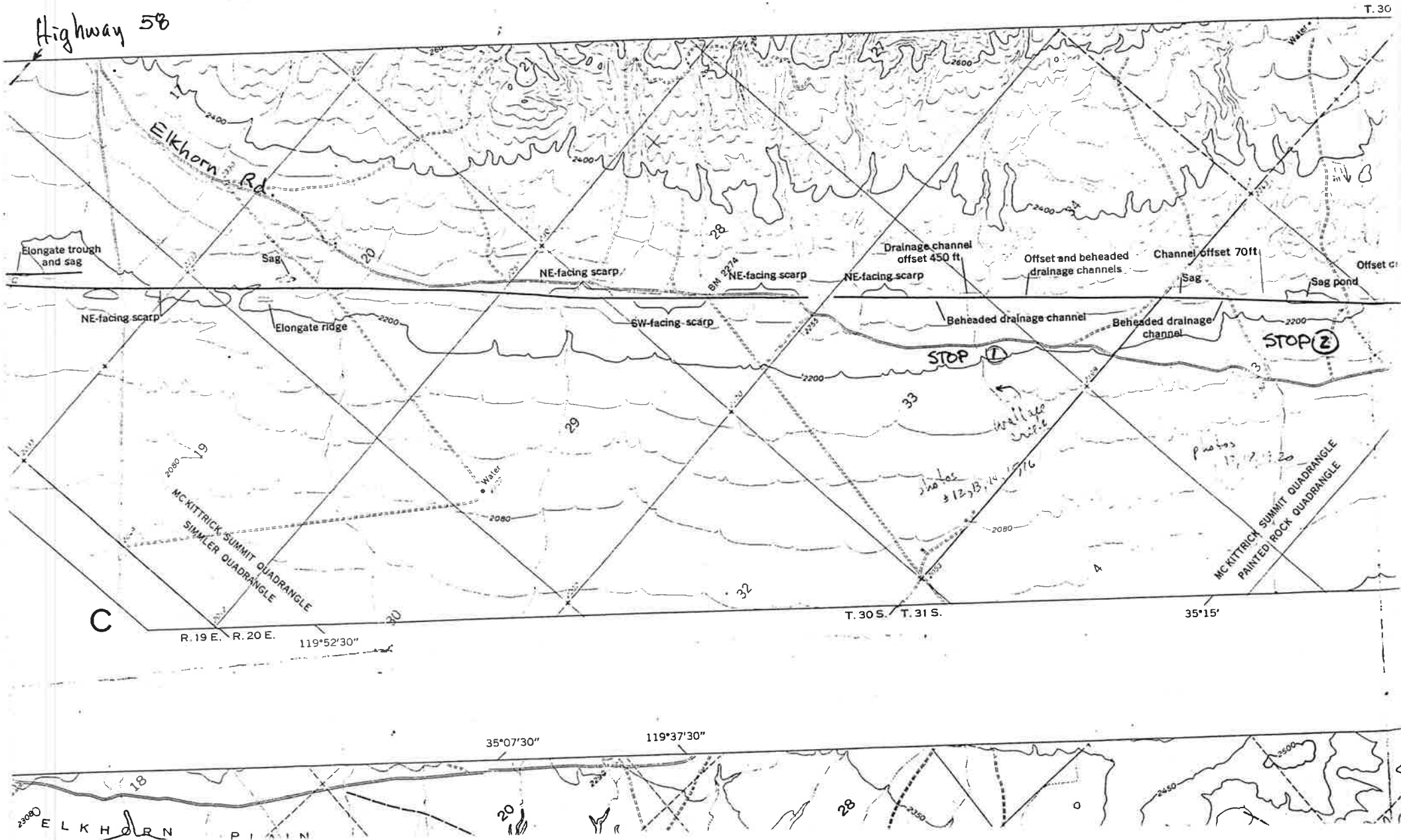
Highway 58
Elkhorn Rd
T. 30
Elongate trough and sag
Sag
NE-facing scarp
BM 2274
NE-facing scarp
NE-facing scarp
Drainage channel offset 450 ft
Offset and beheaded drainage channels
Channel offset 70ft
Sag
Sag pond
NE-facing scarp
Elongate ridge
SW-facing scarp
Beheaded drainage channel
Beheaded drainage channel
STOP 1
STOP 2
Water
McKITTRICK SUMMIT QUADRANGLE
SIMMLER QUADRANGLE
McKITTRICK SUMMIT QUADRANGLE
PAINTED ROCK QUADRANGLE
C
R. 19 E.
R. 20 E.
119°52'30"
T. 30 S.
T. 31 S.
35°15'
35°07'30"
119°37'30"
ELKHORN PLAIN

A CONTRIBUTION OF THE NATIONAL CENTER
FOR EARTHQUAKE RESEARCH

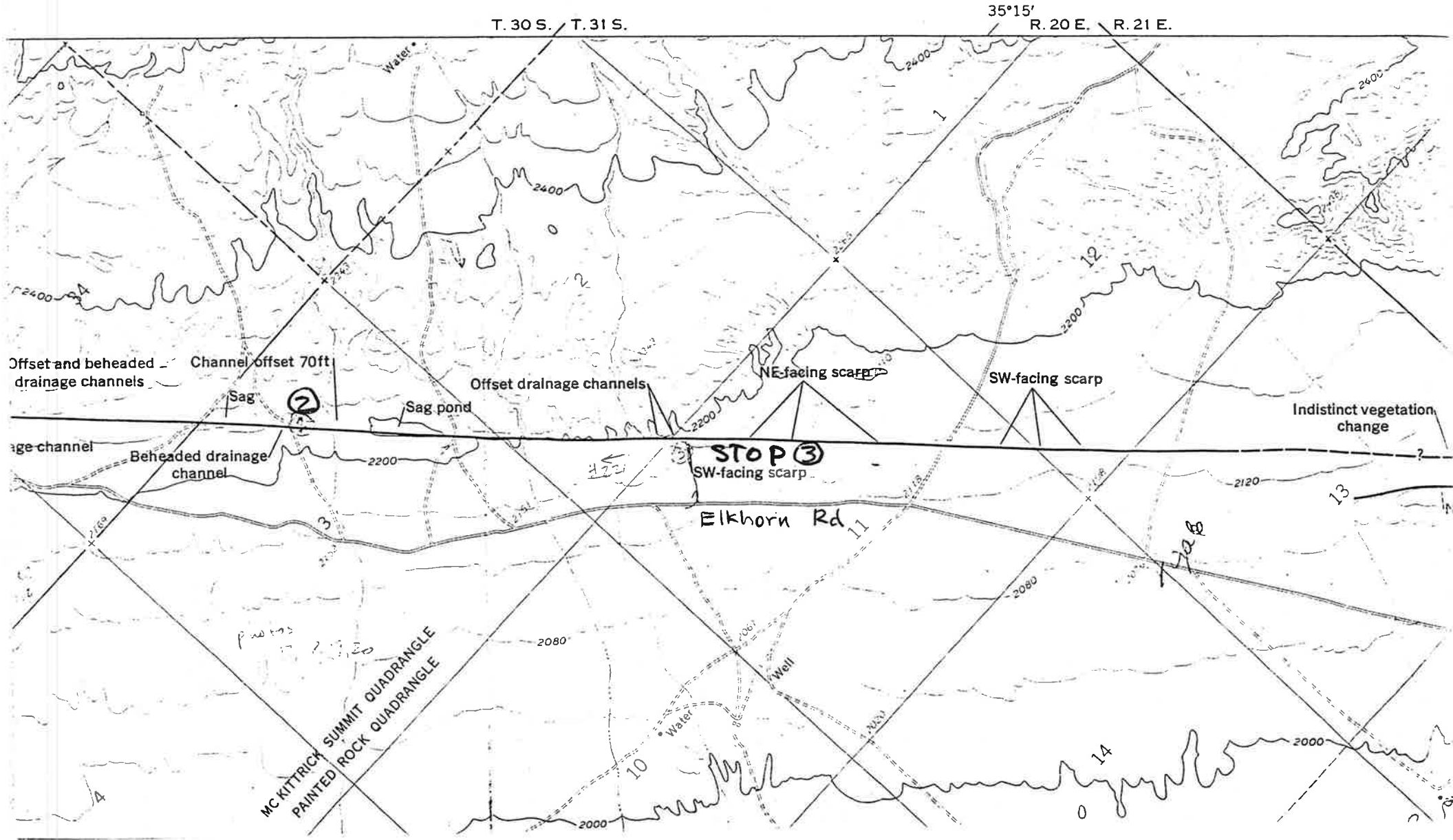

P.O = Photo Opportunity

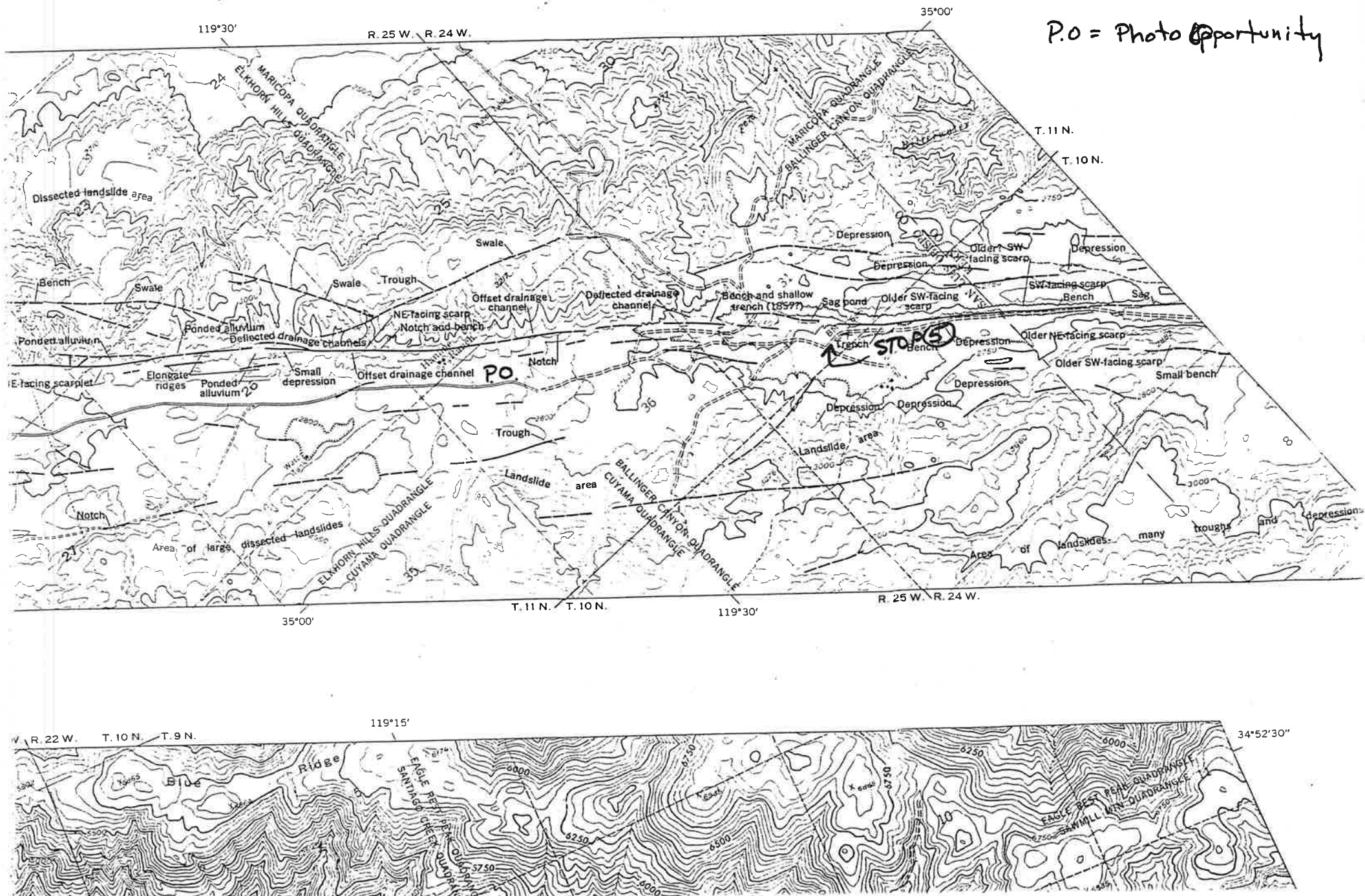

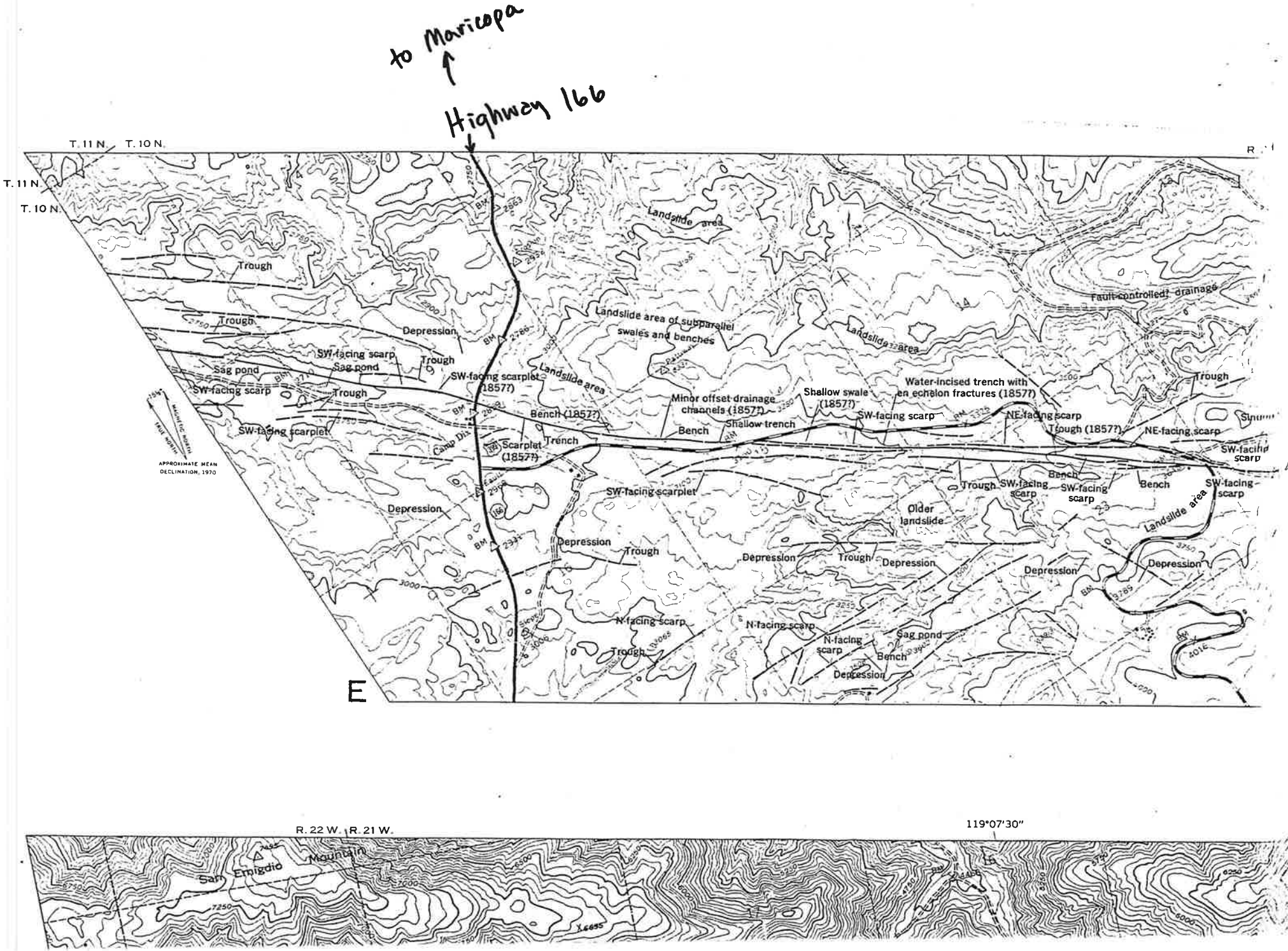
to Maricopa
Highway 166
T. 11 N.
T. 10 N.
R. 22 W.
R. 21 W.
119°07'30"
Trough
Depression
SW-facing scarp
Sag pond
SW-facing scarplet (1857?)
Landslide area
Landslide area of subparallel swales and benches
Fault-controlled? drainage
Water-incised trench with en echelon fractures (1857?)
Minor offset drainage channels (1857?)
Shallow swale (1857?)
Shallow trench
Bench (1857?)
Bench
Scarplet (1857?)
Trench
Camp Dix
NE-facing scarp
Trough (1857?)
SW-facing scarplet
Older landslide
N-facing scarp
Sag pond
Bench
Depression
APPROXIMATE MEAN DECLINATION, 1970
MAGNETIC NORTH
TRUE NORTH
E
San Emigdio Mountain

Holocene activity of the San Andreas fault at Wallace Creek, California

KERRY E. SIEH *Division of Geological and Planetary Sciences, 170-25 California Institute of Technology, Pasadena, California 91125*
RICHARD H. JAHNS* *School of Earth Sciences, Stanford University, Stanford, California 94305*

ABSTRACT

Wallace Creek is an ephemeral stream in central California, the present channel of which displays an offset of 128 m along the San Andreas fault. Geological investigations have elucidated the relatively simple evolution of this channel and related landforms and deposits. This history requires that the average rate of slip along the San Andreas fault has been 33.9 ± 2.9 mm/yr for the past 3,700 yr and 35.8 + 5.4/-4.1 mm/yr for the past 13,250 yr. Small gullies near Wallace Creek record evidence for the amount of dextral slip during the past three great earthquakes. Slip during these great earthquakes ranged from ~9.5 to 12.3 m. Using these values and the average rate of slip during the late Holocene, we estimate that the period of dormancy preceding each of the past 3 great earthquakes was between 240 and 450 yr. This is in marked contrast to the shorter intervals (~150 yr) documented at sites 100 to 300 km to the southeast. These lengthy intervals suggest that a major portion of the San Andreas fault represented by the Wallace Creek site will not generate a great earthquake for at least another 100 yr. The slip rate determined at Wallace Creek enables us to argue, however, that rupture of a 90-km-long segment northwest of Wallace Creek, which sustained as much as 3.5 m of slip in 1857, is likely to generate a major earthquake by the turn of the century.

In addition, we note that the long-term rates of slip at Wallace Creek are indistinguishable from maximum fault-slip rates estimated from geodetic data along the creeping segment of the fault farther north. These historical rates of slip along the creeping reach thus do represent the long-term—that is, millennial—average, and no appreciable elastic strain is accumulating there.

Finally, we note that the Wallace Creek slip rate is appreciably lower than the average rate of slip (56 mm/yr) between the Pacific and North American plates determined for the interval of the past 3 m.y. The discrepancy is due principally to slippage along faults other than the San Andreas, but a slightly lower rate of plate motion during the Holocene epoch cannot be ruled out.

INTRODUCTION

California has experienced many episodes of tectonic activity during the past 200 m.y. During the past 15 m.y. horizontal deformations due to the relative motion of the Pacific and North American plates have been dominant. On land, the major actor in this most recent plate-tectonic drama has been the San Andreas fault, across which ~300 km of right-lateral dislocation has accumulated since the middle Miocene (Hill and Dibblee, 1953; Crowell, 1962, 1981; Nilsen and Link, 1975).

The San Andreas fault traverses most of coastal California, running close to the populous Los Angeles and San Francisco Bay regions (Fig. 1a). Its historical record of occasional great earthquakes (Lawson and others, 1908; Agnew and Sieh, 1978) amply demonstrates that it poses a major natural hazard to inhabitants of these regions. The future behavior of the San Andreas fault thus has long been a topic of great interest to Californians. Interpretations of historical, geodetic, and geologic data have yielded estimates of one century to several centuries for the time between great earthquakes along the fault in the San Francisco Bay region (Reid, 1910; Thatcher, 1975). Geologic data indicate that similar recurrence intervals apply in southern California (Sieh, 1978b, and in press).

The behavior of the San Andreas fault during the past few thousands of years is one of the best clues to its future behavior. Useful forecasts concerning the likelihood or imminence of a great earthquake along the fault will be much more difficult without greater understanding of its behavior during the past several millennia.

In this paper, we present and discuss the geologic history of Wallace Creek, a locality about halfway between San Francisco and Los Angeles that contains much information about the Holocene behavior of the San Andreas fault (Fig. 1a). For the purpose of determining rates of slip in Holocene time, the channel of Wallace Creek offers excellent possibilities. The channel crosses and is offset along a well-defined, linear trace of the San Andreas fault in the Carrizo Plain of central California (Fig. 1b). It is relatively isolated from other large drainages, and, therefore, its history is not complicated by involvement with remnants of other drainages that have been brought into juxtaposition.

The simple geometry of Wallace Creek suggests a simple history of development. Arnold and Johnson (1909) inferred 120 m of offset on the San Andreas fault, because the modern channel of the creek runs along the fault for about that distance. Wallace (1968) also inferred a simple history of offset involving incision of a channel into an alluvial plain, offset of ~250 m, then channel filling and new incision across the fault. The latest dextral offset of 128 m then accumulated. These interpretations are verified and quantified by us in this paper.

STRATIGRAPHY AND GEOMORPHOLOGY

Figure 2 is a geologic map of the Wallace Creek area that is based upon surficial mapping and study of sediments encountered in numerous excavations. The map shows four main geologic units: older fan alluvium (uncolored), younger fan alluvium (green), high-channel alluvium (dark orange), and low-channel alluvium (light orange). A mantle of slope wash and local alluvium, which is extensively burrowed by rodents, overlies most of the deposits. This unit has been mapped (brown) only where it is thicker than ~1 m and does not cover units and relationships that need to be shown on the map.

*Deceased.

Geological Society of America Bulletin, v. 95, p. 883–896, 11 figs., 3 tables, August 1984.

Figure 1. a. Wallace Creek (WC) is along the San Andreas fault (SAF) between Los Angeles (LA) and San Francisco (SF), in the Carrizo Plain of central California. b. This oblique aerial photograph shows the modern channel, which has been offset ~130 m, and an abandoned channel that has been offset ~380 m. An older abandoned channel, indicated by white arrow at left, has been offset ~475 m. Photograph by R. E. Wallace, 17 September 1974. View is northeastward.

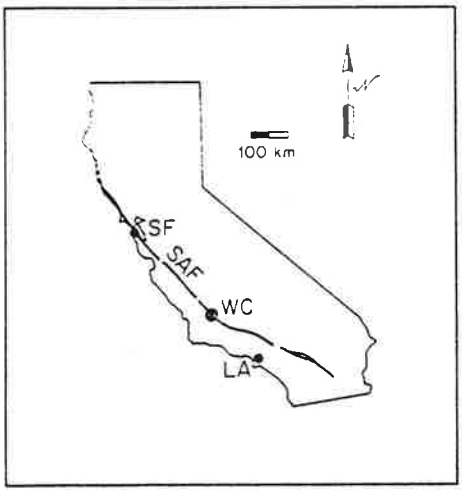

a

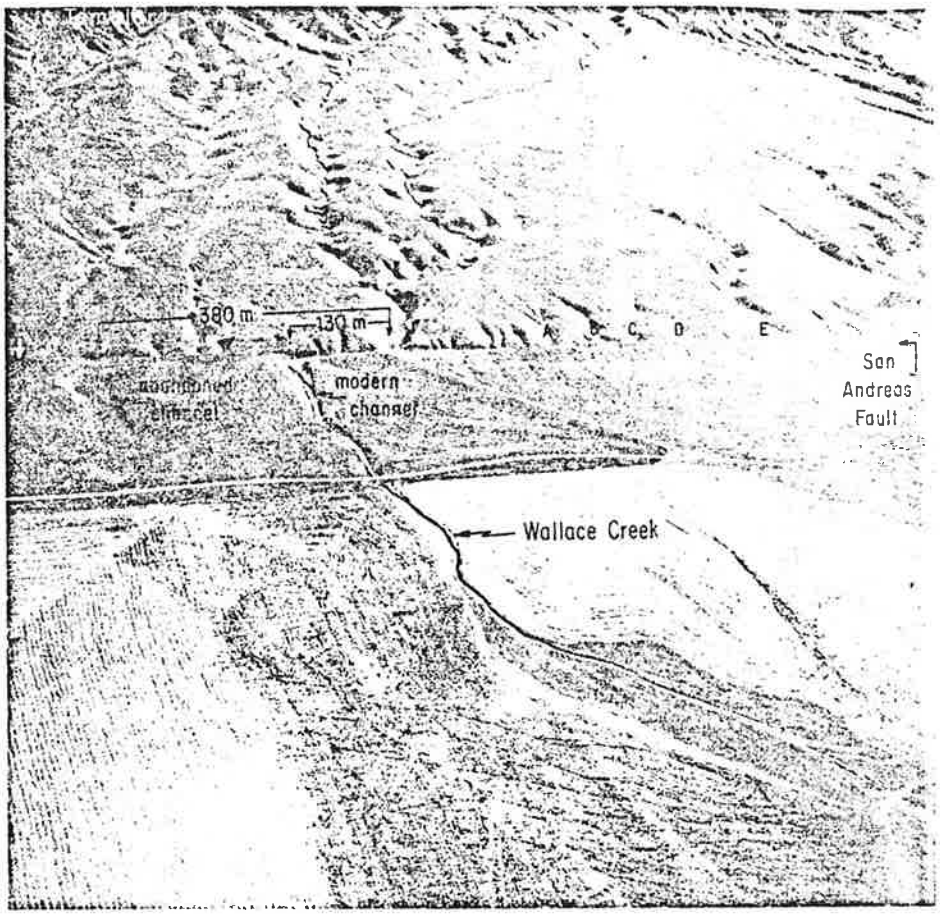

b

Older Fan Alluvium

Underlying all other units exposed at the site, there is a late Pleistocene alluvial fan deposit derived from the Temblor Range to the northeast. This deposit, here termed the "older fan alluvium," consists of thin sheets, lenses, and stringers of indurate silty clay, pebbly sandy clay, and sandy gravel. Most of the trenches (Figs. 2 and 3) exposed this unit. Southwest of the fault, the older fan alluvium is covered by various deposits, but northeast of the fault, the deformed fan surface is incised.

Charcoal disseminated within the older fan alluvium 4 m below the surface of the fan in trench 5 (Fig. 3), yielded an age of 19,340 ± 1,000 yr B.P. (Table 1). The lack of major unconformities and paleosols in the older fan alluvium below or above this dated horizon implies that all of the exposed 13 m of the unit formed during the late Pleistocene epoch. Evidence discussed below supports a conclusion that the fan surface on the northeast side of the fault had become inactive by about 13,000 yr B.P.

FIGURE 2 EXPLANATION

UNITS

- Hl — Low-channel alluvium
- Hh — High-channel alluvium
- Hs — Slope wash (mantles most of area, but mapped only where boundaries are distinct)
- Py — Younger-fan alluvium (dots indicate edges of individual lobes)
- Po — Older-fan alluvium

SYMBOLS

- Contacts (solid where geomorphically apparent or exposed in trench, dotted where buried, dashed where inferred
- 0.3' — Faults (as above; hachures on downthrown side; numbers indicate height of scarp)
- Selected small gullies offset ~9m in 1857
- 5 / 10 — Trenches { backhoe / bulldozer
- Crests of small fans and source gullies offset ~9m in 1857
- 0.3' — Landslide, showing headscarp, scarp height, and direction of movement

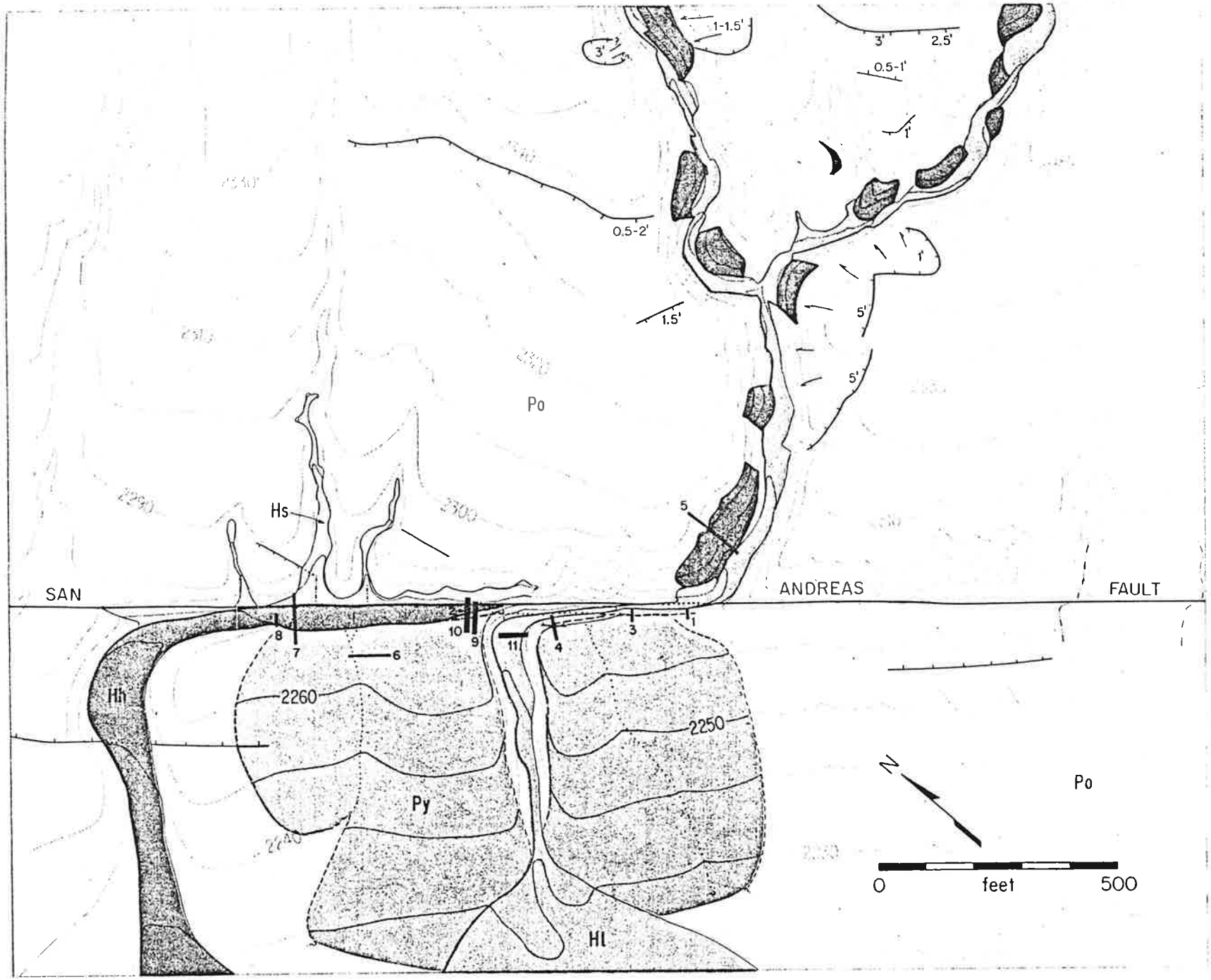

Figure 2. Geologic map of Wallace Creek. Contours of topographic base map show elevation (in feet) above sea level.

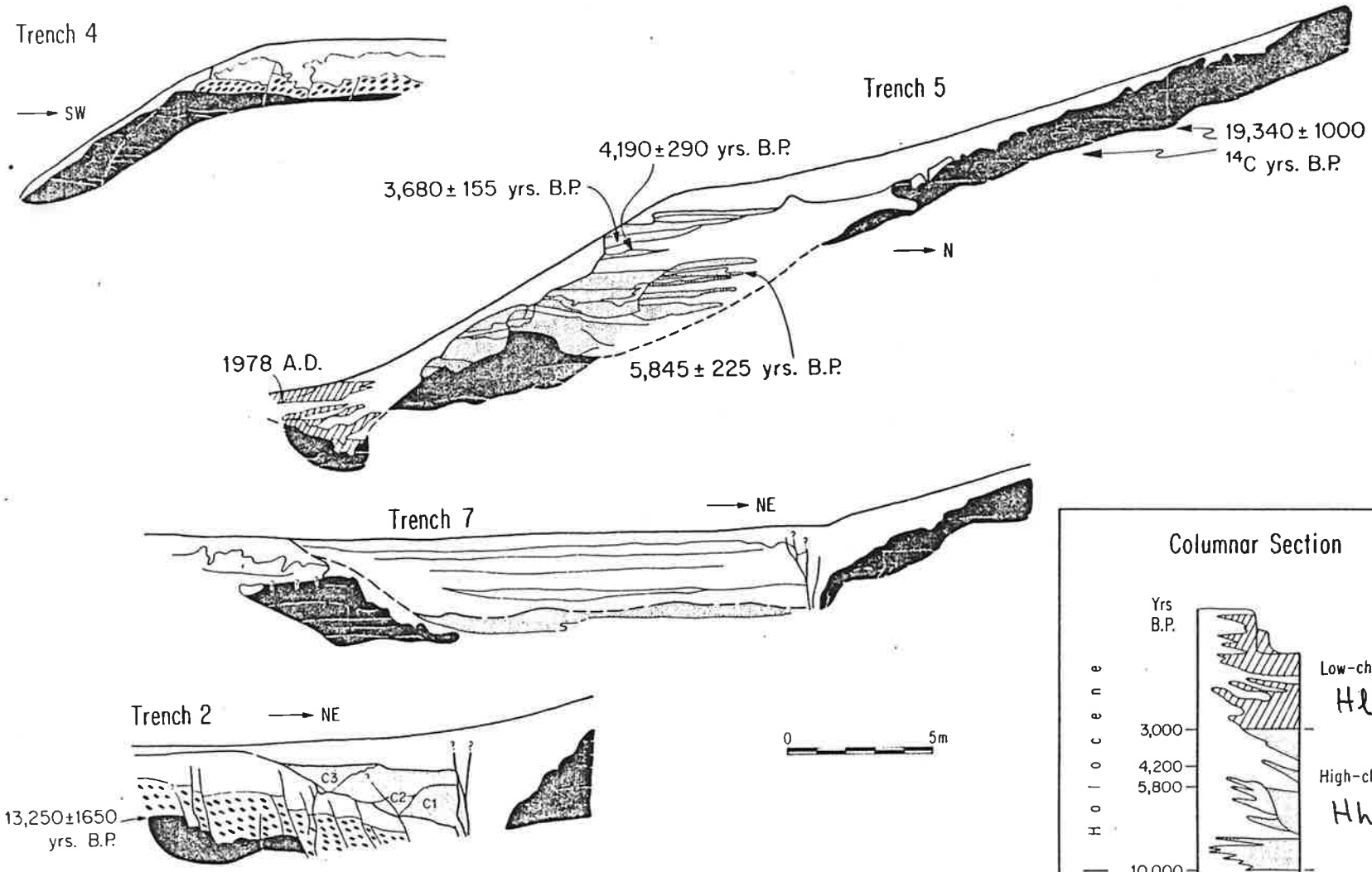

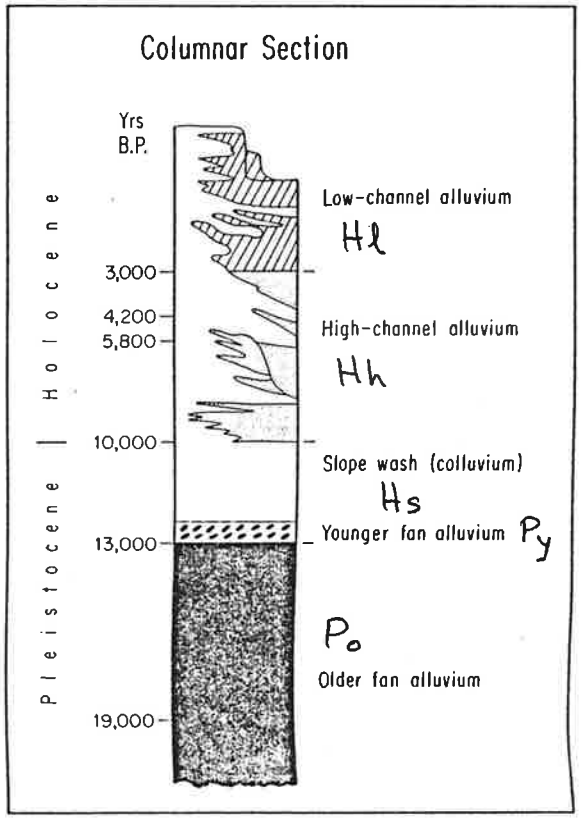

Figure 3. Records of selected excavations at Wallace Creek, California. See Figure 2 for locations. Detailed logs of these and other excavations are available upon request from the author.

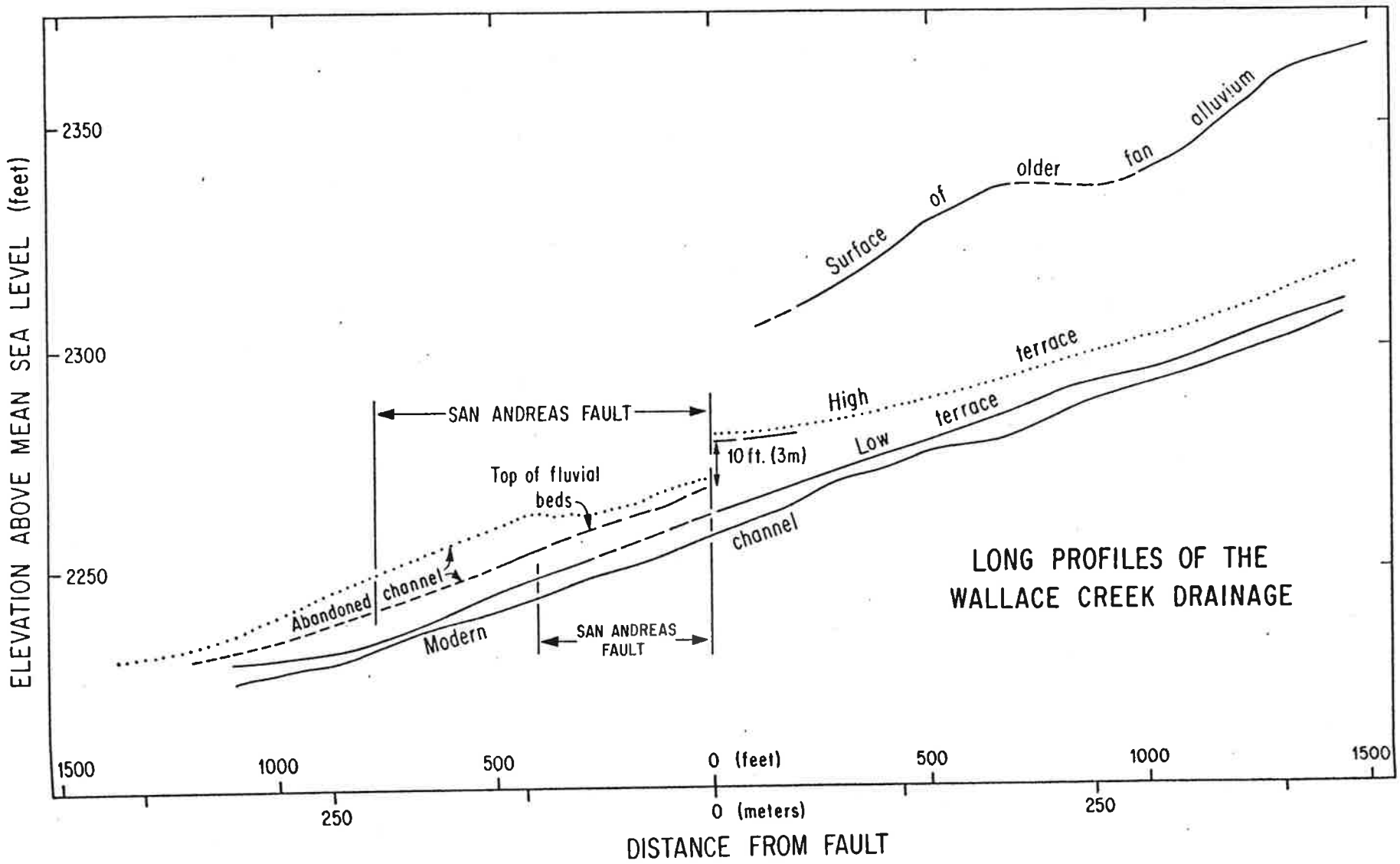

Figure 5. Stream profiles of the modern and the abandoned channels of Wallace Creek. High terrace, indicated by dotted lines, and top of high-channel alluvium, indicated by solid and dashed lines, are offset ~3 m vertically.

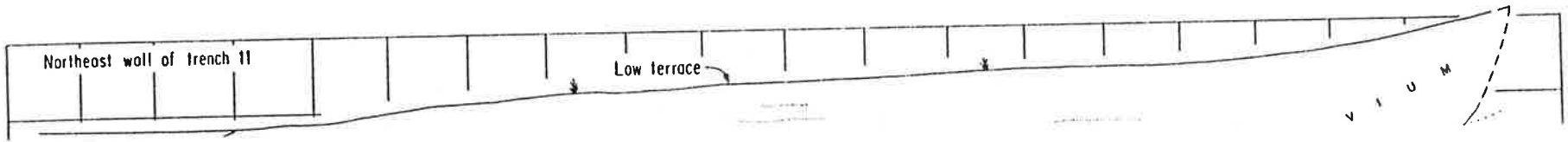

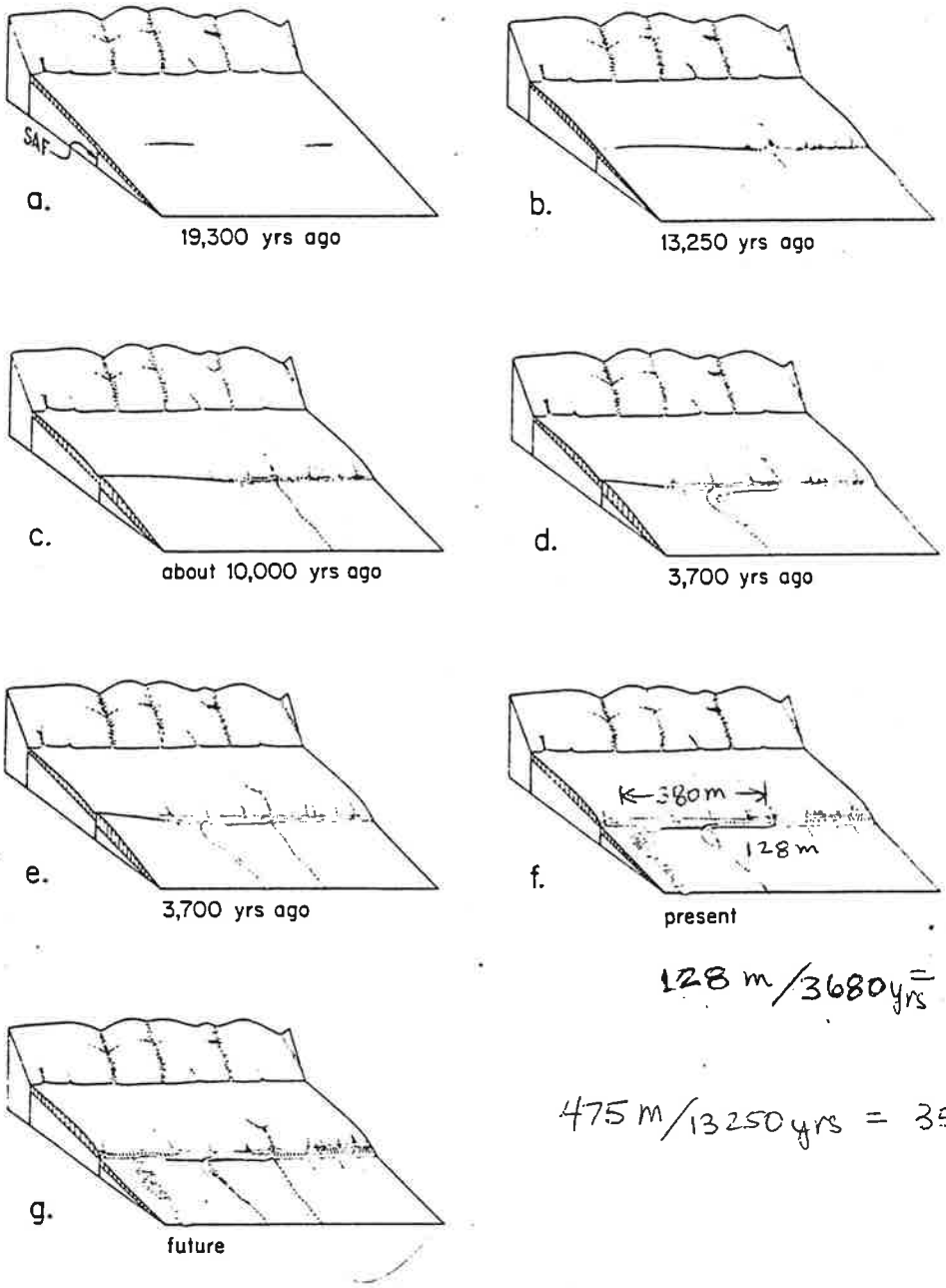

128 m / 3680 yrs = 34.8 mm/yr

475 m / 13250 yrs = 35.8 mm/yr

Figure 7. The Holocene–late Pleistocene evolution of Wallace Creek. An aggrading "older alluvial fan" during the period including 19,300 yr ago progressively buried small scarps formed along the San Andreas fault (SAF) during major strike-slip events (a). Right-lateral offsets accumulated during this period, but no geomorphologically recognizable offsets began to form until 13,250 yr ago, when the "older alluvial fan" became inactivated by initial entrenchment of Wallace Creek (b). At this time, erosion of small gullies to the right (southeast) of Wallace Creek also resulted in deposition of the "younger fan alluvium" downstream from the fault. These features then began to record right-lateral offset, and scarps began to grow along the fault. About 10,000 yr ago, a new channel was cut across the fault at Wallace Creek, and the initial channel, downstream from the fault, was abandoned (c). The new channel remained the active channel of Wallace Creek during the early and middle Holocene, during which ~250 m of slip accumulated (d). This channel filled with "high-channel alluvium" 3,700 yr ago, and Wallace Creek cut a new channel straight across the fault (e). Between 3,700 yr ago and the present, this youngest channel has registered 128 m of right-lateral offset (f). Aggradation of this channel, accompanied by continued offset, will probably lead to its abandonment and the creation of a new channel, cut straight across the fault (g).

(250 + 128)/10,000 = 37.8 mm/year. abandoned channel.
≈ 380 m

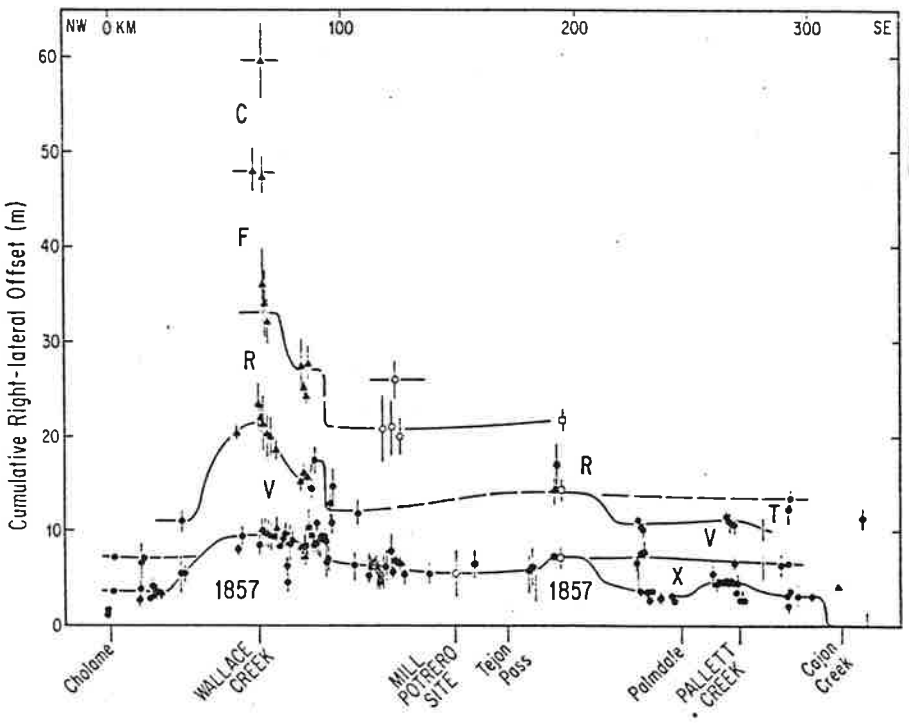

Figure 10. Right-lateral offsets measured along the south-central (1857) segment of the San Andreas fault suggest that slip at each locality is characterized by a particular value. Solid circles are data from Sieh (1978c), with poor-quality data deleted. Open circles are data from Davis (1983). Triangles are new data and remeasurements at sites reported by Sieh (1978c). Open squares are new data. Vertical bars indicate magnitude of imprecision in measurement.

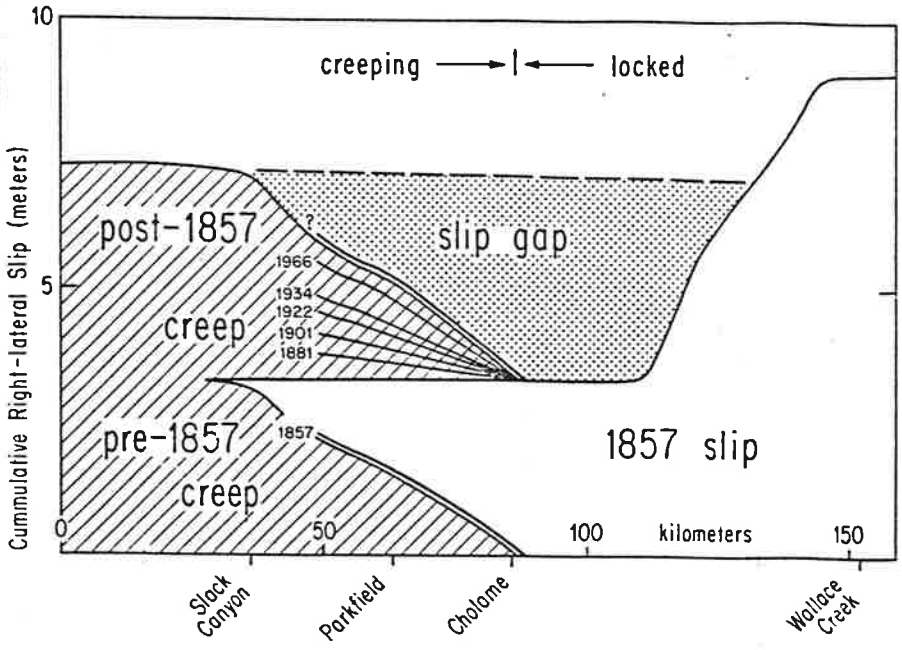

Figure 11. Hypothetical source of future major earthquake along the San Andreas fault includes ~60 km of the currently creeping segment and 30 km of the locked segment. Cumulative right-lateral slip plotted against distance along the fault indicates that this 90-km segment is slip-deficient relative to adjacent stretches of the fault. Slip in 1857 is from Sieh (1978c). Cumulative slip along the creeping segment is extrapolated from alignment array slip rates for period 1968–1979 (Lisowski and Prescott, 1981, Fig. 6). Dates of moderate earthquakes generated by slip along the fault in the Parkfield-Cholame region are shown. because such an event probably triggered the great 1857 rupture and conceivably could trigger the rupture of the slip gap.

TABLE 2. SMALLEST STREAM OFFSETS NEAR WALLACE CREEK AND PROPOSED INTERVALS BETWEEN GREAT EARTHQUAKES

(1) Stream offsets (m)	(2) Remarks	(3) Produced by	(4) Slip associated with earthquake (m)	(5) Proposed interval between events (yr)
9.5 ± 0.5(± 1σ)	Average of 5 measurements	1857 event	9.5 ± 0.5(± 1σ)	
21.8 ± 1.1	Average of 4 measurements**	1857 plus last prehistoric event	12.3 ± 1.2*	240 to 320§
32.8 or 33.5 ± 1.9	Average of 3 measurements**	1857 plus latest 2 prehistoric events	11.0 or 11.7 ± 2.2†	300 to 440§ 240 to 450§

*$21.8 - 9.5 \pm (0.5^2 + 1.1^2)^{1/2}$.
†$32.8 - 21.8 \pm (1.1^2 + 1.9^2)^{1/2}$ or $33.5 - 21.8 \pm (1.1^2 + 1.9^2)^{1/2}$.
§Slip during following earthquake in column 4 divided by average late Holocene slip rate (33.9 ± 2.9 mm/yr).
**Offset gullies are all between Wallace Creek and Gully D in Figure 1.

TABLE 3. SMALLEST STREAM OFFSETS NEAR WALLACE CREEK AND PROPOSED DATES AND CORRELATION OF LATEST FOUR GREAT EARTHQUAKES

(1) Stream offsets (m)	(2) Time required to accumulate offset as elastic strain using average late Holocene slip rate (years)	(3) Proposed dates for latest earthquakes (A.D.)	(4) Possible correlations with events recognized at Pallett Creek	(5) Possible correlations with events recognized at Mill Potrero by Davis (1983)
		1857	Z(1857)	Z(1857)
9.5 ± 0.5 (± 1σ)	240 to 320			
		1540 to 1630*	V(1550 ± 70)	V(1584 ±70)
21.8 ± 1.1	560 to 740			
		1120 to 1300†	R(1080 ± 65)	
32.8 or 33.5 ± 1.9	840 to 1140			
		720 to 1020§	F(845 ± 75)	

*1857 - (240 to 320 yr).
†1857 - (560 to 740 yr).
§1857 - (840 to 1140 yr).

G12-05 1422H

Late Holocene Slip Rate on the Mojave Segment of the San Andreas Fault Zone, Littlerock, CA: Preliminary Results

DAVID P. SCHWARTZ and RAY WELDON, (both at: MS 977, U.S. Geological Survey, Menlo Park, CA 94025)

The Mojave segment of the San Andreas fault zone extends from Tejon Pass to Cajon Pass and contains the southern 145 km of the 1857 surface faulting. Two disparate late Holocene slip rates have been published for sites along this part of the 1857 rupture; 9 mm/yr for the past 1100 years at Pallet Creek (Sieh, 1984) and 46-60 mm/yr for the past 750 to 1000 years near Three Points (Rust, 1982; 1986).

We have recently begun new studies at the 96th St. site near Littlerock, 8-1/2 km northwest of Pallet Creek and 45 km northwest of the junction of the San Andreas and San Jacinto faults. Here, the fault is a well-defined zone 3 to 7 m wide that contains a vertical and a southwest-dipping trace. It offsets an alluvial fill sequence and post-fill pond and colluvial deposits. Charcoal from burn layers date the top of the fill at 1000 to 1200 years B.P. A stream offset of 19 m that post-dates the fill sequence yields a minimum slip rate of 16 to 19 mm/yr. The main fill-bearing channel is offset a maximum of 130 m. Charcoal from within the fill yielded an age of 3510 $\pm$ 220 14C yr B.P. This gives a maximum slip rate on the offset channel of 38 mm/yr. Tentative correlation of offset facies boundaries within the fill sequence suggests the latest Holocene slip rate is in the lower end of the 16 to 38 mm/yr range. A precise slip rate on the Mojave segment is important for evaluating proposed rupture models for the San Andreas fault zone.

Prehistoric Large Earthquakes Produced by Slip on the San Andreas Fault at Pallett Creek, California

KERRY E. SIEH[1]

Geology Department, Stanford University, Stanford, California 94305

Late Holocene marsh deposits composing a terrace about 55 km northeast of Los Angeles, California, contain geologic evidence of many large seismic events produced by slip on the San Andreas fault since the sixth century A.D. I excavated several trenches into the deposits in order to study this evidence. The principal indicators of past events are (1) sandblows and other effects of liquefaction, (2) the termination of secondary faults at distinct levels within the stratigraphic section, and (3) sedimentary deposits and faulted relationships along the main fault. The effects upon the marsh deposits of six of the eight prehistoric events are comparable to those of the great (M_s = 8¼+) 1857 event, which is the youngest of the nine events disturbing the strata and is associated with about 4½ m of right lateral slip nearby. Two large events may be smaller than this. Radiocarbon dates indicate that the events occurred in the nineteenth, eighteenth, fifteenth, thirteenth, late twelfth, tenth, ninth, seventh, and sixth centuries A.D. Recurrence intervals average 160 years but vary from ½ century to about 3 centuries. The dates may indicate a fairly systematic pattern of occurrence of large earthquakes.

1. INTRODUCTION

Background and Purpose

The geologic record of the recent past provides the best opportunities for study of the long-term behavior of active faults, especially in areas that lack a long historical record of seismicity [*Allen*, 1975]. Many of the phenomena that accompany earthquakes are preserved in the sedimentary record. These include faults, folds, fissures, soft sediment deformation, and sandblows. A few geologists have attempted to use such features preserved in young sediments to date prehistoric earthquakes and calculate average recurrence intervals. In an excavation across a fault scarp associated with the 1971 San Fernando earthquake, for example, *Bonilla* [1973] recognized and may have dated an older, buried scarp produced during a previous earthquake, and in excavations of datable prehistoric lake sediments, which were faulted during the 1968 Borrego Mountain earthquake, *Clark et al.* [1973] recognized evidence of many prehistoric events and were able to infer an average recurrence interval for moderate events. Also, *Sims* [1973, 1975] has correlated deformed layers of lake deposits with known historical earthquakes.

I studied a section of late Holocene sediments, broken by the San Andreas fault, in an attempt to characterize certain aspects of the late Holocene slip history of one segment of this large strike slip fault. Specifically, I wished to determine when large prehistoric events had occurred, thereby deriving an understanding of the frequencies and irregularities of their occurrence. Such knowledge of the long-term behavior of the San Andreas fault and other faults would provide a better geologic context in which to interpret possible geophysical precursors to large earthquakes.

Setting

During the period of historical record (i.e., the past 100–200 years) the San Andreas fault has exhibited contrasting styles of behavior between its individual reaches. In general, segments that ruptured in 1857 and 1906 (Figure 1) have been seismically very quiet since their respective great earthquakes. The intervening segment, approximately 100 km in length, has been creeping relatively continuously throughout the twentieth century and is characterized by a high level of seismicity [*Brown and Wallace*, 1968].

Allen [1968] has proposed, on the basis of the rather permanent geological and geometrical characteristics of and contrasts between the creeping and the dormant segments, that the historical behavior is representative of the long-term behavior. This implies that the segments which produced the great 1906 and 1857 earthquakes are characterized by great earthquakes separated by long periods of dormancy. Preliminary examinations of offset channels along the 1857 break seem to support this hypothesis [*Sieh*, 1977, chapter 2], but further study will be necessary to confirm or deny it.

The site of this study is at least 25 km from the southernmost terminus of the fault rupture associated with the great (M_s = 8¼+) 1857 earthquake (Figures 1 and 2) [*Sieh*, 1978]. Offset stream channels indicate that 1857 displacements in the vicinity were between 3 and 4½ m (Figure 2) [*Sieh*, 1978].

Since 1857 the level of seismicity along the fault near the site has been low. Figure 3 shows earthquakes ($M \gtrsim 6$) that have occurred within 80 km of the site. The four smaller events (7, 9, 10, and 11) that have occurred close enough to produce moderate intensities at the site are also plotted. None of the events are believed to have been associated with slip along the trace of the San Andreas fault.

Pallett Creek is an ephemeral stream that flows down the north flank of the San Gabriel mountains and into the Mojave Desert (Figure 4). Near the base of the mountains it flows across the San Andreas fault. Figure 5 illustrates the en echelon configuration of the recent fault traces near Pallett Creek.

For centuries, conditions at this crossing have been favorable for the preservation of the geologic features produced in association with earthquakes. The San Andreas fault has ruptured the sediments repeatedly, and their rapid accumulation has produced stratigraphic separation of the faulting events. Long hiatuses in sedimentation have been infrequent, and scour has not eliminated large portions of the record. An abundance of carbonaceous materials allows radiometric dating of events recorded in the layers. Finally, modern incision of the deposits by Pallett Creek has lowered the water table and exposed the previously saturated deposits.

[1] Now at Division of Geological and Planetary Sciences 170-25, California Institute of Technology, Pasadena, California 91125.

Paper number 8B0461.
0148-0227/78/088B-0461$01.00

JOURNAL OF GEOPHYSICAL RESEARCH, VOL. 89, NO. B9, PAGES 7641–7670, SEPTEMBER 10, 1984

Lateral Offsets and Revised Dates of Large Prehistoric Earthquakes at Pallett Creek, Southern California

KERRY E. SIEH

Division of Geological and Planetary Sciences, California Institute of Technology, Pasadena

Recent excavation and new radiocarbon dates of sediments at Pallett Creek are the basis for new conclusions regarding the late Holocene history of the San Andreas fault. Systematic dissection of a 50-m-long, 15-m-wide, 5-m-deep volume of earth, centered on the fault, enables documentation in three dimensions of fault patterns, lateral offsets, and vertical deformation associated with large earthquakes of the past. The excavations expose evidence for 12 earthquakes that occurred between about 260 and 1857 A.D., with an average recurrence interval of about 145 years. Prehistoric slip events that occurred in 1720 ± 50, 1550 ± 70, 1350 ± 50, 1080 ± 65, and 845 ± 75 A.D. have lateral offsets that are comparable to those of the most recent great earthquake of 1857. Thus all of these events represent earthquakes of large magnitude. The lateral offsets of two other events, in 935 ± 85 and 1015 ± 100 A.D., are an order of magnitude smaller and may be interpreted in several ways with regard to the size of these events. The new data constrain the average recurrence interval for large earthquakes at this site to between 145 and 200 years but suggest a monotonic decrease in individual intervals to below this range during the past 900 years. On the basis of these data, the probability of a large earthquake with surficial fault rupture at this site is between 0.2 and 5% during 1984 and 7 and 60% by the year 2000.

1. INTRODUCTION

Several years ago I described evidence and reported dates for eight large earthquakes that occurred in the 1300 years before 1857 A.D., the date of the latest great earthquake in southern California [*Sieh*, 1978*a*]. These events were revealed in excavations across the San Andreas fault at Pallett Creek, about 55 km northeast of downtown Los Angeles (Figure 1*a*). Using several radiocarbon (^{14}C) age determinations for various faulted late Holocene layers, I estimated an average recurrence interval of about 160 years between these nine events.

Several limitations plagued the early study at Pallett Creek. First, large uncertainties in the radiocarbon dates translated into large uncertainties for the dates of the individual earthquakes. Thus one could not assess whether variations in recurrence intervals were due to the imprecision of the radiocarbon analyses or to actual variations in the length of time between earthquakes. Second, the sizes of the individual events were difficult to assess because right-lateral dislocations associated with each event could not be measured in the few, isolated, narrow trenches excavated for that study. I did use vertical deformational patterns to assess the size of each prehistoric event relative to the 1857 event, but this involved the assumption that deformation in the vertical plane has occurred in the same proportion to that in the horizontal plane during each of the earthquakes.

In this paper I present new radiocarbon dates and recalculate the date of each earthquake. I also report new measurements of horizontal fault slip associated with most of the earthquakes. In order to reassess the dates of each earthquake recorded at Pallett Creek, I collected additional samples of peat and charcoal from various stratigraphic horizons. Dates from these samples were used in combination with those I reported earlier [*Sieh*, 1978*a*] to recalculate the dates of each earthquake. In addition, excavation of trenches well below the base of the earlier trenches enabled identification and dating of three older earthquakes that had not been known. To determine lateral offsets associated with the large earthquakes at Pallett Creek, I systematically excavated a volume of earth that is roughly 50 m long parallel to the fault, ≥15 m wide, and 5 m deep (Figure 1*c*). Most of the data from the excavated volume come from about 50 vertical exposures oriented nearly at right angles to the fault. Excavation began with a 2-m-wide, 2-m-deep, 20-m-long swath cut across the fault. The two walls of this cut were cleaned, and several points on each wall were located with respect to a reference grid that had been surveyed by transit, rod, and tape prior to excavation. A string grid composed of 1-m squares was then constructed on each exposure (e.g., Figures 2 and 3). The stratigraphy and structure of each square was then documented by color photographs and written descriptions of strikes and dips as well as unit thicknesses, textures, and colors. Documentation of each major exposure required approximately half a day.

Once the walls of the initial excavation were documented, the cut was widened. In this manner the initial exposures were destroyed, but a fresh wall was exposed. After documentation of this new exposure was completed, the excavation was widened further to expose yet another vertical surface. After the first 2-m-deep tier was 10 m or so wide, excavations to a lower, 4-m-deep tier were undertaken. Figures 2 and 3 illustrate walls exposed in the two tiers. In most critical areas the spacing between the mapped vertical exposures was <1 m, and in a few places small horizontal surfaces were prepared and mapped. Documentation of more than 130 exposures within the excavated volume required two summer field seasons (1979 and 1980).

Taken together, the exposure records constitute a three-dimensional latticework of structural and stratigraphic information. Throughout the latticework are major and minor faults and fissures; sandblows, anticlines, synclines, and monoclines; and mappable variations in the textures, colors, and thicknesses of units (for example, see Figures 2 and 3). Dozens of offsets and deformations of various ages are apparent at various levels. Although a large volume of geological record was destroyed in the process of collecting these data, volumes several times as large remain unexcavated within the flood-

Paper number 4B0612.
0148-0227/84/004B-0612$05.00

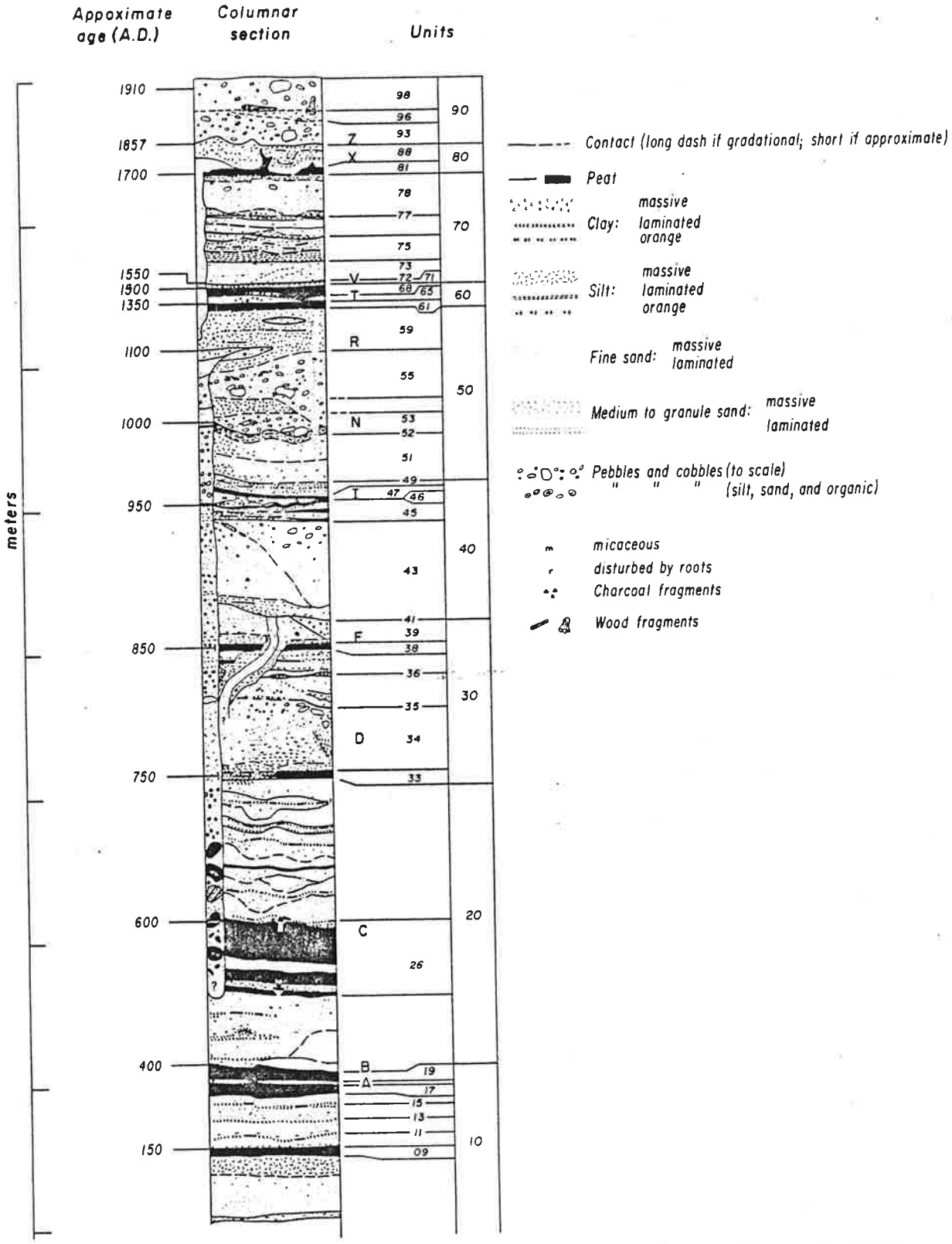

Fig. 4. Generalized columnar section of the late Holocene sediments of Pallett Creek within the excavation. Individual beds are labeled numerically as by *Sieh* [1978*a*]. Each capital letter rests upon the stratum that constituted the ground surface at the time of a particular earthquake. Dates based on radiocarbon analyses are rounded to nearest 50 years.

main rupture locations relative to the reference lines reveals that earlier events involved rupture on more northeasterly planes than later events.

The section that follows makes extensive use of isopach and structure contour maps. Figure 5 illustrates how such maps help determine the vertical deformations associated with particular earthquakes. Isopach maps have proven especially useful in defining the style and magnitude of deformation for

y underlying or overlying bed alone (e.g., events X, d A). Table 2 lists the earthquake dates derived in

evidence of a long hiatus in deposition (centrations, stone lines due to bioturbation, aeolian deflation, or other erosive contacts).

Figure 15 shows each radiocarbon date pl

TABLE 2. Estimated Dates of Latest 12 Earthquakes at Pallett Creek

Event	Date,[a] A.D.	Remarks
Z	1857	Historically documented.
X	1720 ± 50	Unit 81 date is within period from 140 to 305 years B.P.[b] (i.e., 1730 ± 80 A.D.); event occurs at top of unit, so ~20 years must be added to unit 81 date[c], thus 1750 ± 80 A.D.; historical record precludes event after 1769, thus 1720 ± 50 A.D.
V	1550 ± 70	Weighted average of upper unit 68 (1405–1630 = 1518 ± 112 A.D.) and unit 72 (1485–1660 = 1573 ± 88 A.D.), which bracket the earthquake horizon.
T	1350 ± 50	Unit 61 date is within period from 1280 to 1380 (i.e., 1330 ± 50 A.D.); event occurs at top of unit, so ~20 years must be added to unit 61 date, thus 1350 ± 50 A.D.
R	1080 ± 65	Weighted average of samples PC-223a, PC-28, and PC-207c, which bracket the earthquake horizon.
N	870 ± 130	Unit 52 date is within period from 720 to 980 A.D. (i.e., 850 ± 130 A.D.); event occurs at top of unit, so ~20 years must be added to unit 52 date[c], thus 870 ± 130 A.D.
I	1010 ± 115	Weighted average of unit 47 (905–1185 = 1045 ± 140 A.D.) and unit 45 (710–1145 = 930 ± 210 A.D.), which bracket the earthquake horizon.
F	1015 ± 115	Weighted average of unit 41 (695–1220 = 960 ± 265 A.D.) and unit 38 (900–1150 = 1025 ± 125 A.D.), which bracket the earthquake horizon.
D	630 ± 80	Weighted average of unit 36 (435–705 = 570 ± 135 A.D.) and unit 33 (560–750 = 655 ± 95 A.D.), which bracket the earthquake horizon.
C	640 ± 65	Average of two dates for upper unit 26 is 640 ± 65 A.D. Earthquake horizon is within this unit.
B	305 ± 95	Average of 2 dates for upper unit 19 is 305 ± 95 A.D. Earthquake horizon is capped by this unit.
A	135 ± 105	Upper unit 17 date is within period from 20 to 225 A.D. (125 ± 105 A.D.). Event occurs at top of unit, so add 10 years[c].

[a]Rounded to nearest 5 years; error limits are about 95% confidence level.
[b]B.P. is Before Present. Present is defined as 1950 A.D.
[c]See *Sieh* [1978*a*, pp. 3932–3933].

collection of minor faults within the excavation may reasonably be allowed a couple of millimeters per year. The most prominent example of this is the minor fault in Plate 3, panel 19, which experienced 1.5 m of right-lateral slip between 1000 and 1857 A.D. Thus this fault contributed about 2 mm/yr of slip for the period 1000–1857 A. D. Several secondary faults and fissures in the northwestern and southeastern sectors of the site could have experienced a few tens of centimeters of strike slip during events V, X, and Z (Plate 1, panel X and Z and panel V). This much slip would not be readily apparent in the isopach and structure contour maps (Plates 2 and 5) used to determine the larger offsets because the spacing of the excavations used to make these maps was generally 1–2 m across these secondary features. One could hypothesize, for example,

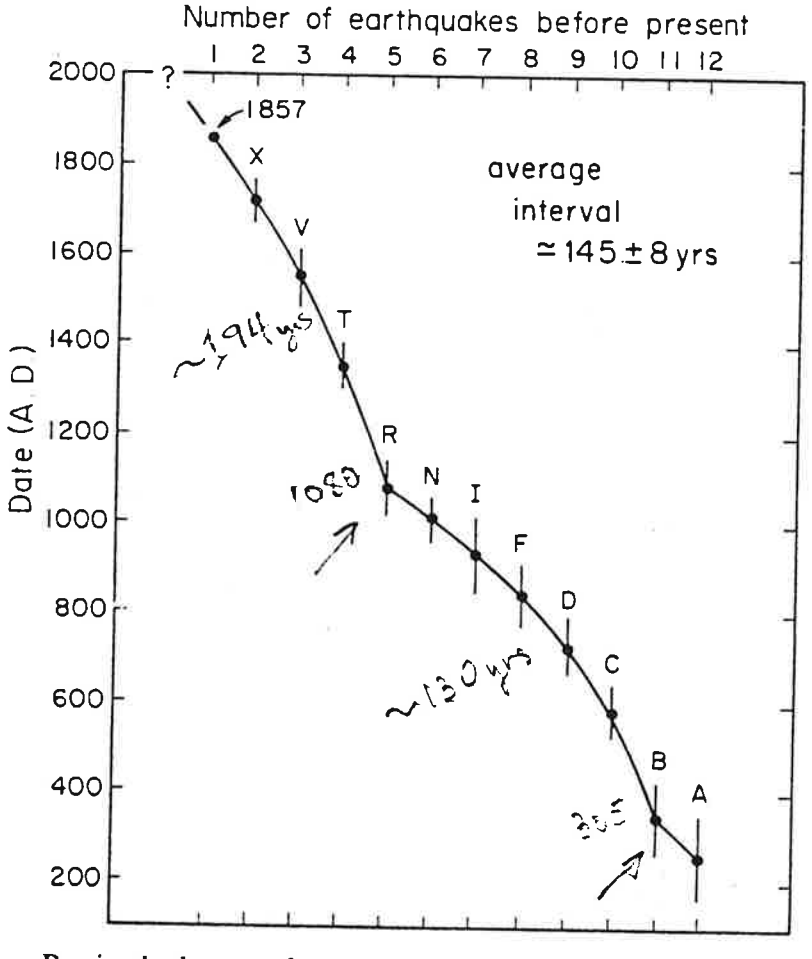

Fig. 16. Revised dates of each earthquake at Pallett Creek. See Tables 2 and 3 for listing of dates.

pected to be appreciа
stepover.

Taken together, min
of the site could conc
mm/yr of right-lateral s
slip rate up to the level
and southeast. Howeve
to account adequately f

5.2. *Average Recurrer*

Various ambiguities
Pallett Creek data wit
terval. Reasonable inte
constrain the average re
between about 145 anc
potheses that provide t
discussion.

The average recurren
quakes identified at Pal
This value is derived s
earliest event, A (261 ±
A.D.), and dividing by t
is 19 years less than wa
smaller set of data. The
uncertainty in the value
of the range of individu
intervals, in fact, seem t
about two and a half cen

The average interval
average interval for larg
seen at Pallett Creek wer
are indeed discernable in
two possibilities need to
sured lateral offsets we
events (Z, X, V, T, and F
quakes. Events D, C, and
offsets associated with ev
two events were large, a
and N represent large eve
imity of Pallett Creek.

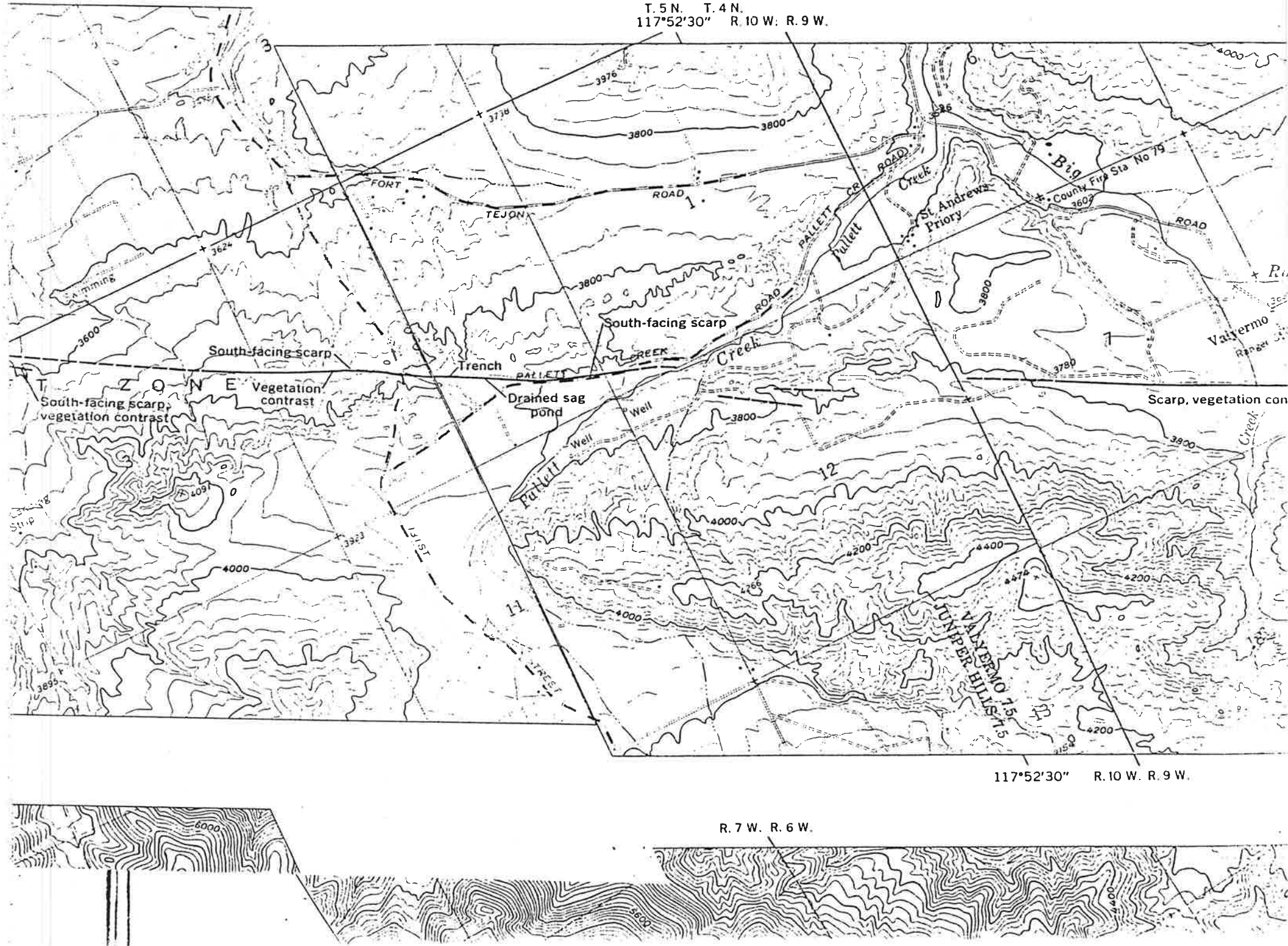
T. 5 N. T. 4 N.
117°52'30" R. 10 W. R. 9 W.
South-facing scarp
South-facing scarp
Trench
Vegetation contrast
South-facing scarp, vegetation contrast
Drained sag pond
Scarp, vegetation con
Pallett Creek
Pallett Creek
Big Creek
FORT TEJON ROAD
PALLETT CR ROAD
ROAD
St. Andrews Priory
County Fire Sta No 79
Valyermo
Well
Well
JUNIPER HILLS 7.5'
VALYERMO 7.5'
117°52'30" R. 10 W. R. 9 W.
R. 7 W. R. 6 W.

successful and has achieved levels of immunity up to 89 per cent in the rat and 70 per cent in the mouse. Similar work shows that non-surface proteins can also be protective and these include an antigen of M_r 97K which, from the sequence of the cloned gene, is identified as schistosome paramyosin.

The genes encoding the M_r 28K and 38K surface antigens and a gene encoding a 25K antigen present in the surface membrane of adult worms and lung-stage parasites have all been cloned in *Escherichia coli*. Two of these genes have also been inserted into vaccinia virus and their immunogenicity is under investigation. It appears that various molecules are potential vaccine candidates but it is likely that a 'cocktail' of antigens providing protection throughout the migratory phase of the life cycle will turn out to be the most effective candidate.

Clearly, progress in providing the molecular basis for a schistosome vaccine is now rapid and follows the lead the malaria field. Indeed, several problems of malaria are not found with schistosomiasis. For example, the schistosome does not multiply within the vertebrate host and therefore a completely effective vaccine may not be essential.

Unlike human malaria, schistosomes infecting man can be grown readily in experimental animals, facilitating the direct testing of a vaccine. Finally, the problem of antigenic diversity and variation, a feature of malaria infections, does not apply to schistosomes, where surface antigens appear to be highly conserved within a species. □

S.R. Smithers is head of the Parasitology Division, National Institute of Medical Research, Mill Hill, London NW7 1AA, UK.

Geophysics

Causes of heating on the San Andreas fault

from Roger N. Anderson

WHAT is happening to the frictional heat that should be produced by the high stresses and movement of the San Andreas fault? Fascinating new results from the first deep measurements by Lachenbruch and his colleagues[1] in a 2-km oil company dry hole between Los Angeles and Barstow have at last shown a 40–50 per cent increase in vertical heat flow near the fault (see figure). This may be the extra heat that was expected from friction along a high-stress fault, but which was not found even after dozens of shallow measurements. But the heat flow is nonetheless puzzling, as it seems considerably lower in the surface sedimentary rocks than in the underlying granite.

There are certainly good grounds for expecting an increased heat flow. Frictional faulting theory and laboratory-derived coefficients of friction indicate high-strength crustal rocks. Large stresses of more than 1,000 atmospheres (1 kilobar) should be required to move rock along a transform fault such as the San Andreas. In support of these laboratory tests, Zoback[2] and colleagues had conducted numerous measurements to 1 km depth that suggest that indeed high stresses exist at shallow depths along the San Andreas fault. Such large stresses, if they can be extrapolated to depth, would produce enough frictional heat along the fault zone to produce a large and easily measurable heat flow anomaly, so it is reassuring that such has now been found, at least at depth.

The problem is how to explain the differential heat flows between the basement granite and the sediment above it. New observations show the profile of temperature against depth in the oil-company hole to be completely uniform and straight.

Heat flow is deduced from indirect measurements of thermal conductivity, which suggest that the sediment is considerably less thermally conductive than the basement. With the same temperature gradient in both structures, the heat flow must be less in the sediment than the basement, and either horizontal hydrothermal flow is carrying heat away near the boundary (which is only a few feet thick) or thermal refraction from steeply dipping

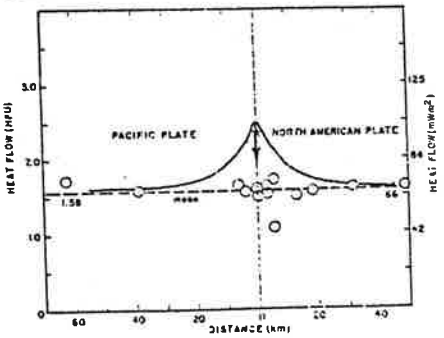

Heat flow versus distance away from the San Andreas fault. High-stress fault zone models predict high heat flow (solid line). The mean heat flow across the fault is flat (dashed line). Non-equilibrium, high heat flow at the fault, which is detected in a 2-km hole in basement granite, is indicated by the star. Corrections caused by complexities at the site may decrease the value in the direction of the arrow. Adapted from data in ref. 5.

contacts between the granite and sediment in deflecting the heat.

The argument thus puts a question mark over the calculations of thermal conductivity, but these are difficult to budge. First, geophysical logs[3] indicated that the sediment — which is itself made of weathered granite — has 20 per cent porosity; and second, measurements of electrical conductivity show that the basement rock is twice as electrically resistive as the sediment. Only fresh water, filling the porosity in the sediment, is electrically conducting enough to explain the difference. The assumption of 20 per cent fresh water then brings the calculated thermal conductivity of the sediment well below that of the basement.

It thus appears that the heat flow around the oil well is complex, possibly suffering from local disturbances. The region is certainly geologically complex. The hole is in a mountain pass, and Ray Weldon of the US Geological Survey has shown from careful, skilful geological mapping[4] in the area that about 1 km of sediment has been eroded from the well site in the past million years. Calculations by Lachenbruch show that this amount of rapid erosion could cause some, but probably not all, of the anomalously high heat flow in the granite.

The question now is what is happening to heat flow, and the supposed high stress in the fault, even deeper than the 2 km presently drilled. Luckily, observations at those depths may soon be to hand. Some while ago, Mark Zoback proposed to drill a new 5 km hole at the site of the oil-company hole at a time when the 'heat flow anomaly' was the total absence of frictional heating.

Now, this deeper hole, to begin in 1987, seems even more imperative. Zoback will lead a team of 27 scientists from 7 universities and US Geological Survey in making geophysical and geochemical measurements in the hole, which is to be sponsored by the US National Science Foundation programme for the deep observtion and sampling of the Earth's continental crust (DOSECC).

The DOSECC programme will also receive core which will be made available for general study by scientists, in much the same fashion as the Ocean Drilling Program supplies its deep-sea cores. Only this deep work below the apparent 'disequilibrium zone' at the drill site seems likely to provide the deep measures of stress and heat flow near the San Andreas fault that are now required. □

1. Lachenbruch, A. *et al. EOS* 67, 379 (1986).
2. Zoback, M. *et al. EOS* 67, 371 (1986).
3. Anderson, R. *EOS* 67, 379 (1986).
4. Weldon, R. *EOS* 67, 380 (1986).
5. Lachenbruch, A. & Sass, J. *J. geophys. Res.* 85, 6185 (1980).

Roger N. Anderson is at the Lamont-Doherty Geological Observatory, Palisades, New York 10964, USA.

Holocene rate of slip and tentative recurrence interval for large earthquakes on the San Andreas fault, Cajon Pass, southern California

RAY J. WELDON II*
KERRY E. SIEH
} *Division of Geological and Planetary Sciences, California Institute of Technology, Pasadena, California 91125*

ABSTRACT

Detailed mapping of the San Andreas fault zone, where it crosses Cajon Creek in Southern California, has revealed a number of late Quaternary deposits and geomorphological features offset by the fault. Radiocarbon dating of these alluvial and swamp deposits has provided a detailed chronology with which to characterize the activity of the San Andreas fault.

Four independent determinations of the slip rate on the San Andreas fault yield an average rate of 24.5 ± 3.5 mm/yr for the past 14,400 yr. The similarity of the four values, which span different intervals of time from 5,900 to 14,400 yr ago, suggests that the slip rate has been constant during this period. The sum of the Holocene slip rate on the San Andreas (~24.5 mm/yr) and the Quaternary rate on the San Jacinto (~10 mm/yr) faults southeast of their junction is the same as the Holocene slip rate on the San Andreas farther northwest (~34 mm/yr). Although the slip rate confirms that the San Andreas fault is accumulating slip faster than any other fault of the plate boundary, a large fraction of the plate boundary's rate of slip (~20 of 56 mm/yr) cannot be accounted for on major faults in southern California.

An excavation has provided evidence for at least 2 earthquakes, and perhaps as many as 4, that caused rupture on the fault between 1290 and 1805 A.D.; it has provided tentative evidence for 6 earthquakes in about the past 1,000 yr. Both lines of evidence suggest an average recurrence interval for large earthquakes of ~1½ to 2 centuries. Combined with the historic record, this investigation indicates that the last major earthquake at Cajon Creek was probably near the beginning of the 18th century.

Models consistent with the record at Cajon Creek and data from other localities along the San Andreas fault have been constructed to estimate the timing and rupture length for future earthquakes on the San Andreas fault.

INTRODUCTION

This paper addresses the late Quaternary rate of slip on the San Andreas fault and provides evidence for the recurrence interval of large earthquakes at Cajon Creek (CC, Fig. 1), ~60 mi east of Los Angeles. Progressive offset of radiocarbon dated, late Pleistocene and Holocene deposits and landforms by the San Andreas fault yields a set of slip rates spanning the past 14,400 yr. An excavation provides evidence for the timing of recent earthquakes. The study area, which is southeast of the junction of the San Andreas and San Jacinto faults, provides data for comparing the activities of these two major faults in southern California.

Fourteen radiocarbon (^{14}C) dates (Table 1) were obtained from charcoal, peat, and aragonitic gastropod shells collected from alluvial deposits and a swamp developed on several terraces formed by Cajon Creek and its major tributary, Lone Pine Creek. Horizontal offsets were measured on terrace risers, buried channels, small streams incised across the fault, and landslides. Vertical offsets were determined by comparing the levels of geomorphological surfaces across the fault after restoring the lateral motion.

The key to determining the slip rate and the tentative recurrence interval was to integrate the landforms and deposits into a coherent history of interaction between the faulting and the depositional and erosional processes active in the area. The fluctuation of Cajon Creek between periods of deposition and erosion resulted in the major deposits and landforms which preserve

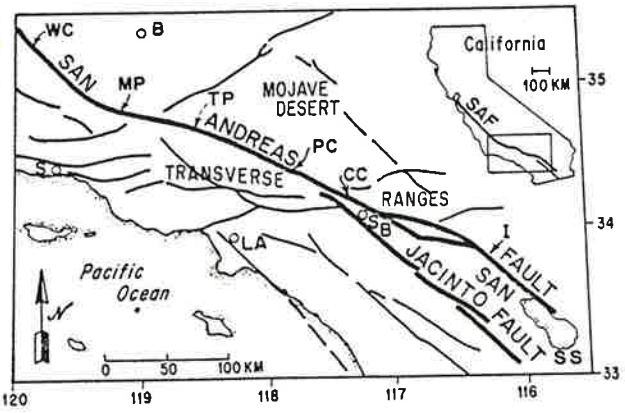

Figure 1. Index map of southern California showing the major faults. The study area, Cajon Creek, is indicated by CC. Other localities mentioned in the text are Wallace Creek (WC), Mill Potrero (MP), Pallett Creek (PC), and Indio (I). Los Angeles (LA), San Bernardino (SB), Santa Barbara (S), Bakersfield (B), and the Salton Sea (SS) are indicated for reference.

*Present address: Occidental College, Los Angeles, California 90041, and U.S. Geological Survey, Menlo Park, California 94025.

Additional material for this article may be secured free of charge by requesting Supplementary Data 85-20 from the GSA Documents Secretary.

Geological Society of America Bulletin, v. 96, p. 793–812, 15 figs., 1 table, June 1985.

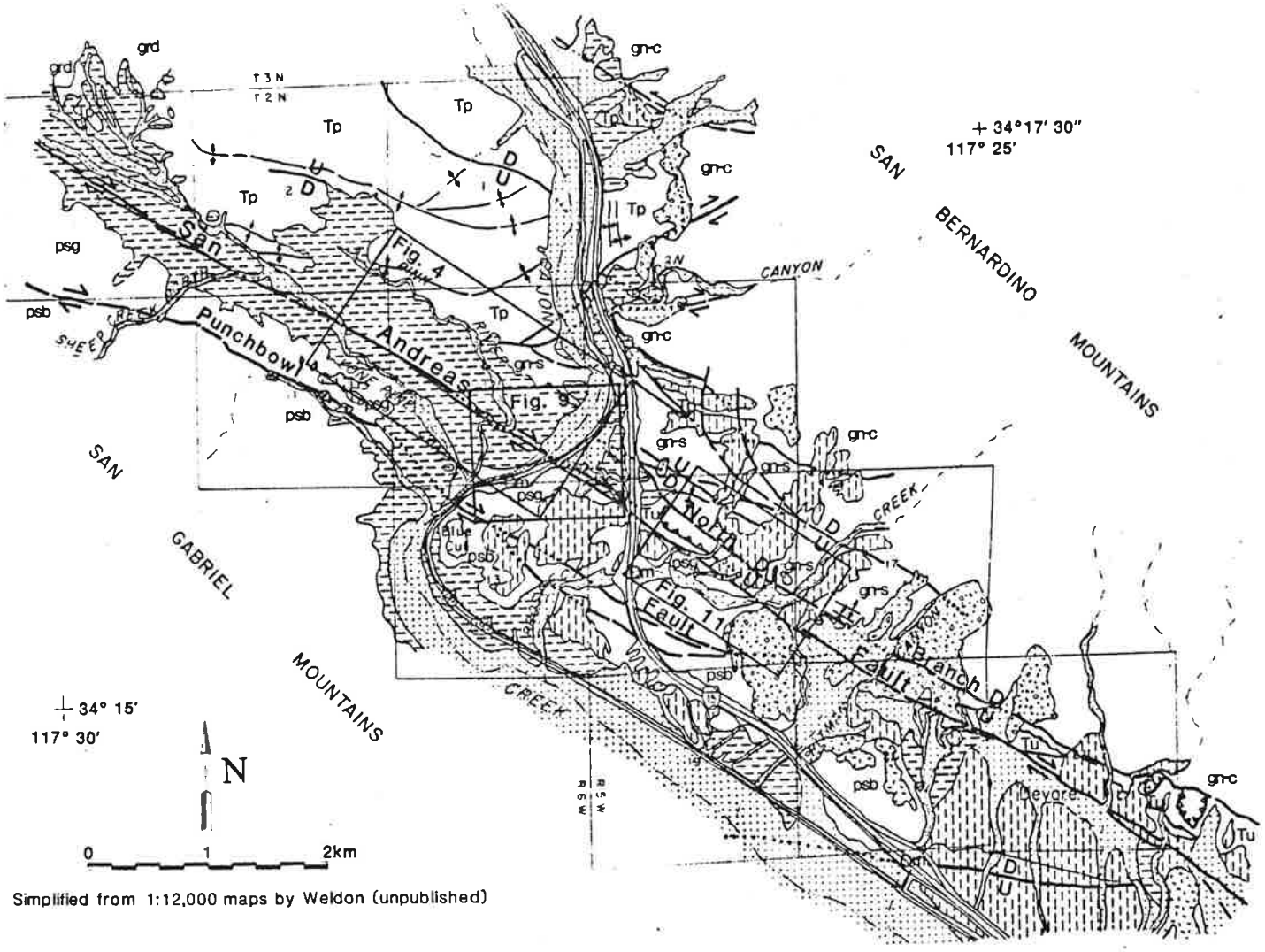

Figure 2. Geologic map of the study area emphasizing the Quaternary geology. The locations of more detailed maps are indicated by boxes.

EXPLANATION FOR FIGURE 2

Fault, solid where certain, dashed where inferred, dotted where buried, and a thrust where barbed.

Depositional contact, dashed where inferred.

Fold hinge, arrows indicate sense of dip.

Holocene alluvium: includes Qal, Qal-0, Qoa-a, and, locally, Qhf (see text and explanations for other figures).

Qoa-c: latest Pleistocene alluvium, 14.8 to 12.4 ka.

Major landslides and, locally, colluvium.

Qoa-d: late Pleistocene alluvium, ~55 ka.

Qoa-e: middle Pleistocene alluvium, ~500 ka.

Qm Man-made fill.

Tp Punchbowl Formation (Cajon facies).

grd Granodiorite, underlies the Punchbowl Formation.

gn-c Gneiss, granodiorite to tonalite, and Crowder Formation. This package underlies the San Bernardino Mountains.

gn-s Gneiss, overlain by latest Cretaceous San Francisquito Formation(?); relation to gn-c not clear.

Tu Unnamed Tertiary(?) conglomerates and sandstone, overlies and faulted against quartz monzonite; only crops out between the North Branch and the San Andreas faults.

psg Pelona Schist: "green facies," mainly albite-epidote-chlorite schist; only crops out between the Punchbowl and San Andreas faults.

psb Pelona Schist: "blue facies," mainly micaceous quartzofeldspathic schist; underlies much of the San Gabriel Mountains southwest of the Punchbowl fault.

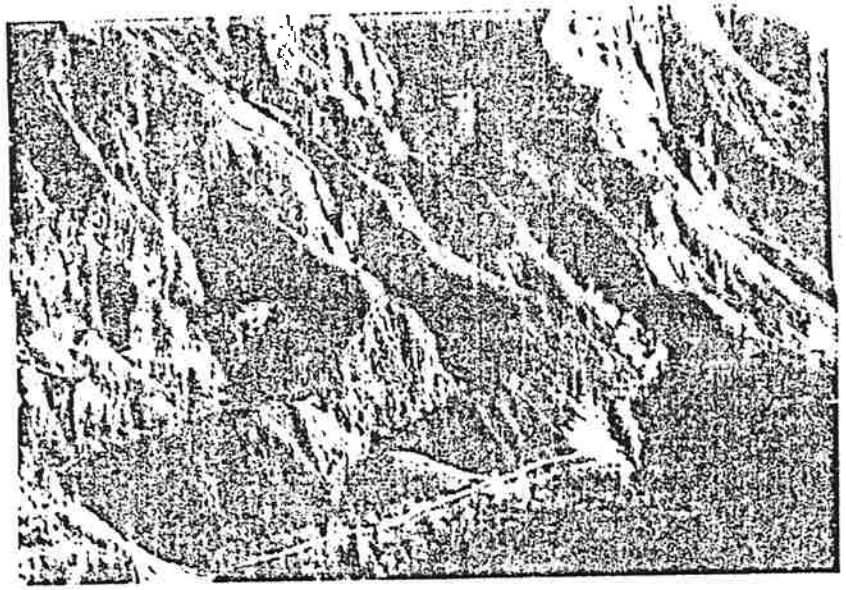

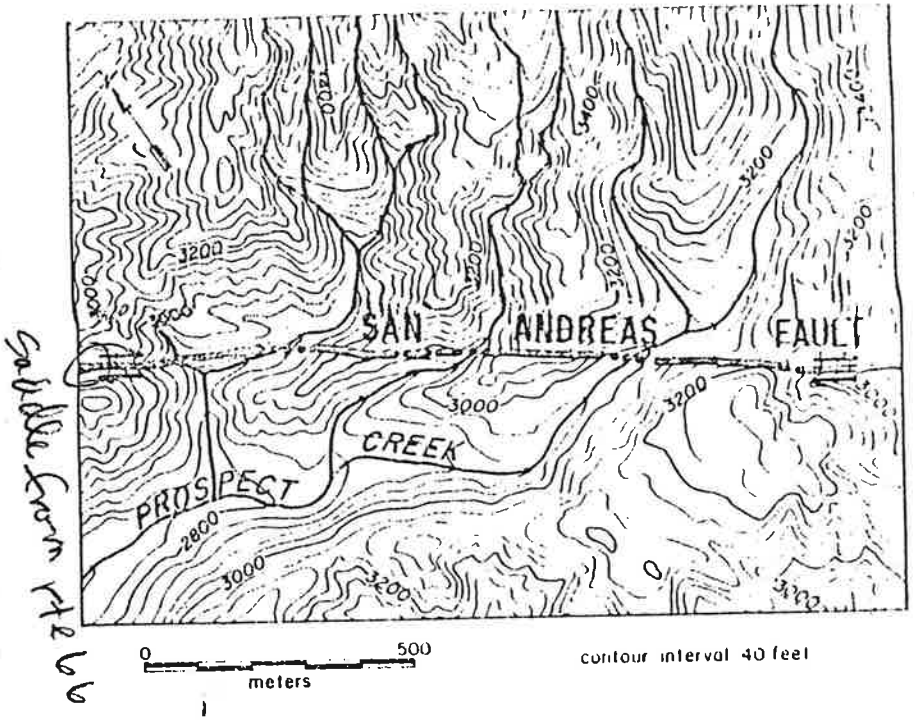

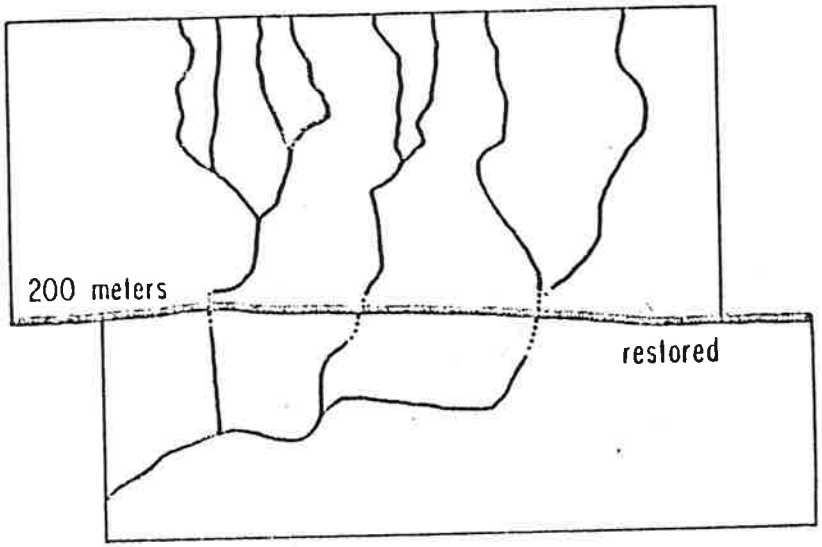

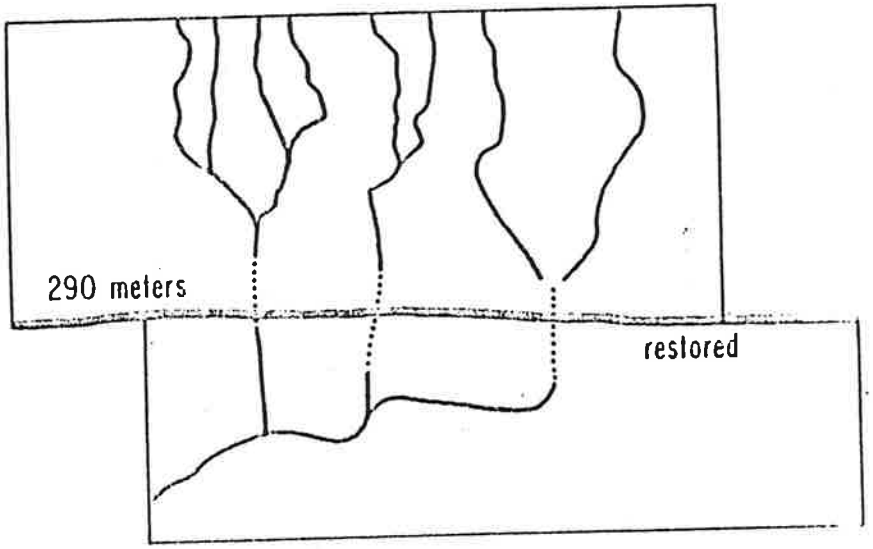

Figure 11. Offset of the tributaries of Prospect Creek. The 290-m offset of each of the streams is inferred to have begun when Cajon Creek (and its tributaries) incised after the deposition of Qoa-c. The matches are both based on the westernmost stream, which has a deeply incised channel on both sides of the fault. The 200-m restoration is based on the "inner gorge" offset that probably relates to renewed incision following Qt-3.

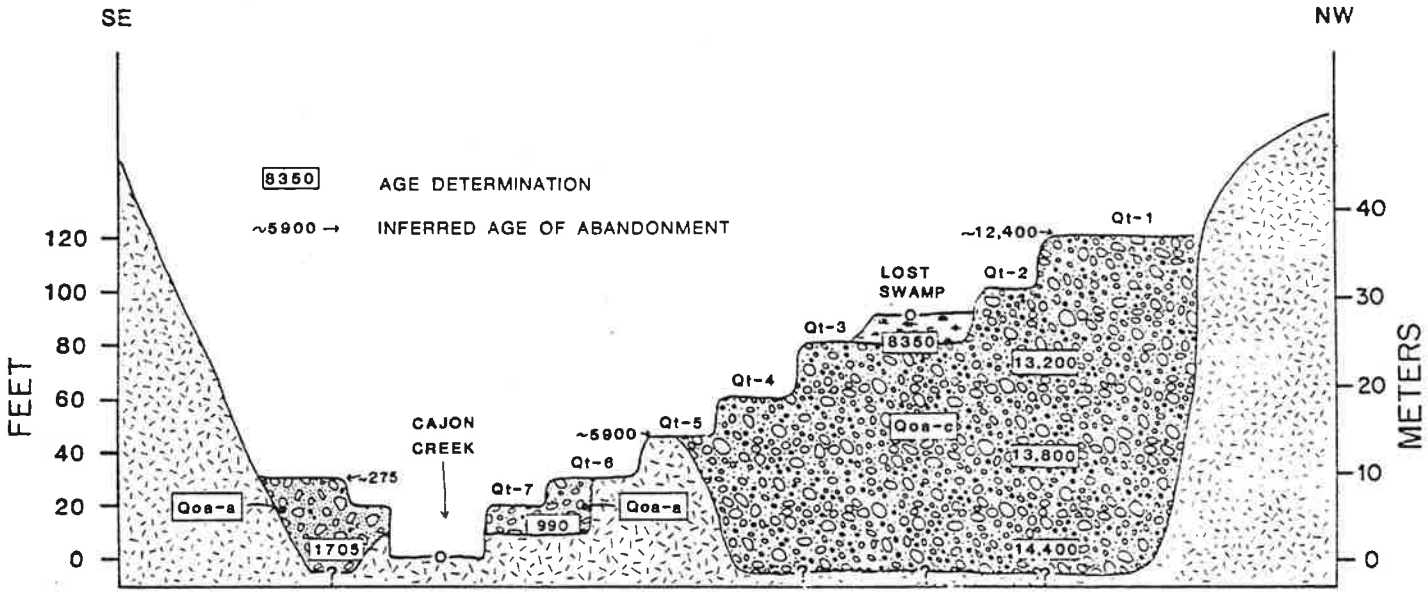

Figure 3. Schematic section through Cajon Creek. The section is parallel to the San Andreas fault south of the fault with Qt-2, Qt-3, Qt-4, and Lost Swamp added from Lone Pine Canyon. Radiocarbon dates from up and down the creek and from Lost Swamp are in approximate stratigraphic position (boxes). The abandonment ages of Qt-1, Qt-3, Qt-5, and Qt-6 (dates without boxes are extrapolations) are based on relating the stratigraphy to geomorphic events (see text). Notice that Qoa-c and Qoa-a extend below the current level of Cajon Creek and indicate earlier periods of deeper incision.

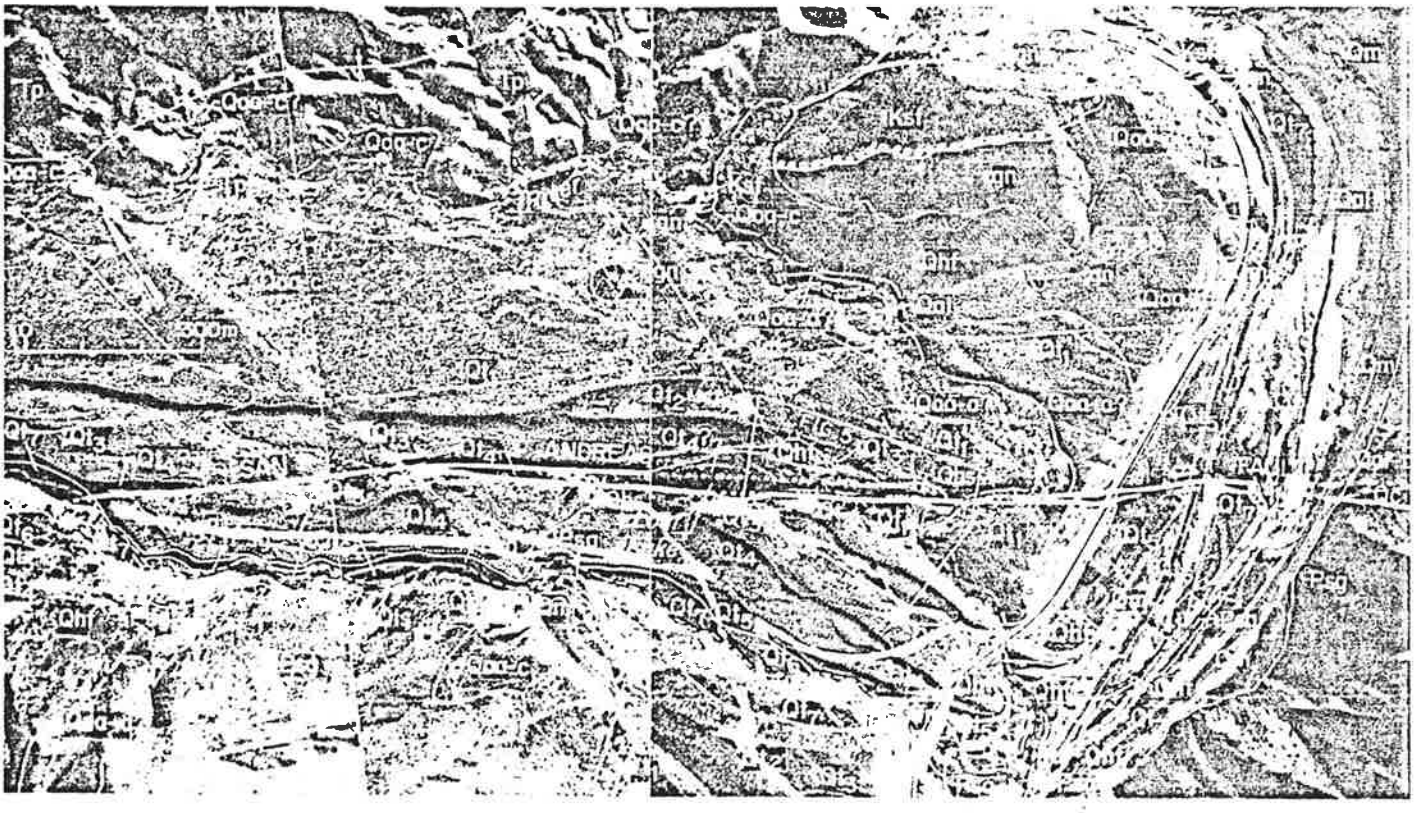

Figure 4. Airphoto mosaic of the Lost Lake area. Stratigraphic and geomorphic units are annotated in white. The northwest-trending terrace risers between the terraces cast shadows on the northeast side of the river and are brightly illuminated on the southwest side. The offsets of Pink River, Qt-3 (near Lost Swamp), and Qt-5 (at Cajon Creek) are well illustrated, as is the contrast between the fault and the sinuous river terraces. The younger terraces are less well defined, both in width and level, and are more numerous near the junction of Lone Pine and Cajon Creeks.

EXPLANATION FOR FIGURE 4

Depositional contact, solid where certain, dashed where inferred or uncertain, and dotted where buried; contains circles for a distinct basal conglomerate.

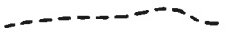

Limit of present drainage.

Fold hinge, with direction of plunge; arrows indicate syncline or anticline.

Geomorphic contact, dashed where inferred or uncertain; designates the edge of a surface where it is not a geologic contact; where two surfaces meet it is the edge of the upper one (top of riser). Note that a geomorphic contact can cross a geologic contact where a geomorphic surface is developed across more than one geologic unit.

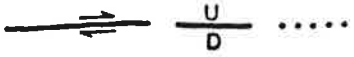

Fault, solid where certain, dashed where inferred, and dotted where buried.

QUATERNARY UNITS

1982 A.D.	Qal	Current alluvium.
	Qhs	Active swamp; underlain by sediments that span most of the Holocene.
	Qhf	Fanglomerates; locally includes material deposited continuously since the Pleistocene.
	Qc	Colluvium (where distinguished), commonly transitional into Qhf or Qoa.
	Qm	Man-made fill (where distinguished).
1938 A.D.	Qal-0	Alluvium deposited by the 1938 flood (where distinguished).
200 yr B.P.	Qt_7	Youngest strath mapped.
275–1705 B.P.	Qoa-a (Qt_6)	Holocene alluvium; Qt_6 is the surface formed by the top of the Qoa-a deposit.
5900 yr B.P.	Qt_5	Youngest strath recognized above the Qoa-a fill.
	Qt_4	Strath terrace, probably underlies Lost Lake.
8350 yr B.P.	Qt_3	Only Holocene strath widely recognized outside the Lost Lake area; Qt_3 underlies most of Lost Swamp.
	Qt_2	Oldest strath between Qoa-a and Qoa-c.
12.4 to 14.8 ka	Qoa-c (Qt_1)	Latest Pleistocene alluvium; Qt_1 is the surface of the deposit.
	Qls	Landslide.
53–57 ka	Qoa-d	Middle Wisconsin alluvium.
500 ka	Qoa-e	Old red alluvium; deeply weathered with, locally, several meters of brick-red soil.

PRE-QUATERNARY UNITS

Middle to late Miocene	Tp	Punchbowl Formation (Cajon beds). Buff to pink, continental arkosic sandstone and conglomerate.
Late Cretaceous to Eocene(?)	Ksf	San Francisquito Formation. Marine sand and siltstone overlying gn. Has a coarse basal conglomerate of mainly local clasts (indicated by small circles).
≥ Middle Tertiary	Psb	Blue facies, Pelona schist; low-grade metasedimentary marine(?) rocks; only occurs southwest of the Punchbowl fault.
≥ Middle Tertiary	Psg	Green facies, Pelona schist; low-grade, albite-epidote-chlorite metavolcanics and calcareous metasediments; only occurs northeast of the Punchbowl fault.
≥ Late Cretaceous	gn	Undifferentiated gneiss. Heterogeneous, generally tonalitic, foliated, and locally banded rocks. Consists of at least two distinct terranes (not distinguished here).

been offset ~1¼ km. This "inner gorge" is recognized in most of the major drainages in the area and appears to represent a regional climatic event (Weldon, 1983). Several strath terraces produced during this incision are only locally preserved within the inner gorge and add little to the fluvial or tectonic history. The incision probably had ended by 25 ka and certainly was complete by 14.8 ka, when the deposition of Qoa-c (the next youngest deposit) began. The 25-ka estimate is based on the observation that the large landslide near Pitman Canyon (Fig. 2) buries a topography more deeply incised than is the modern topography. The landslide's offset of ~615 m and the slip rate of 24.5 mm/yr are used to estimate its age.

The oldest alluvial deposit in the inner gorge is Qoa-c (Fig. 3). Six radiocarbon samples have

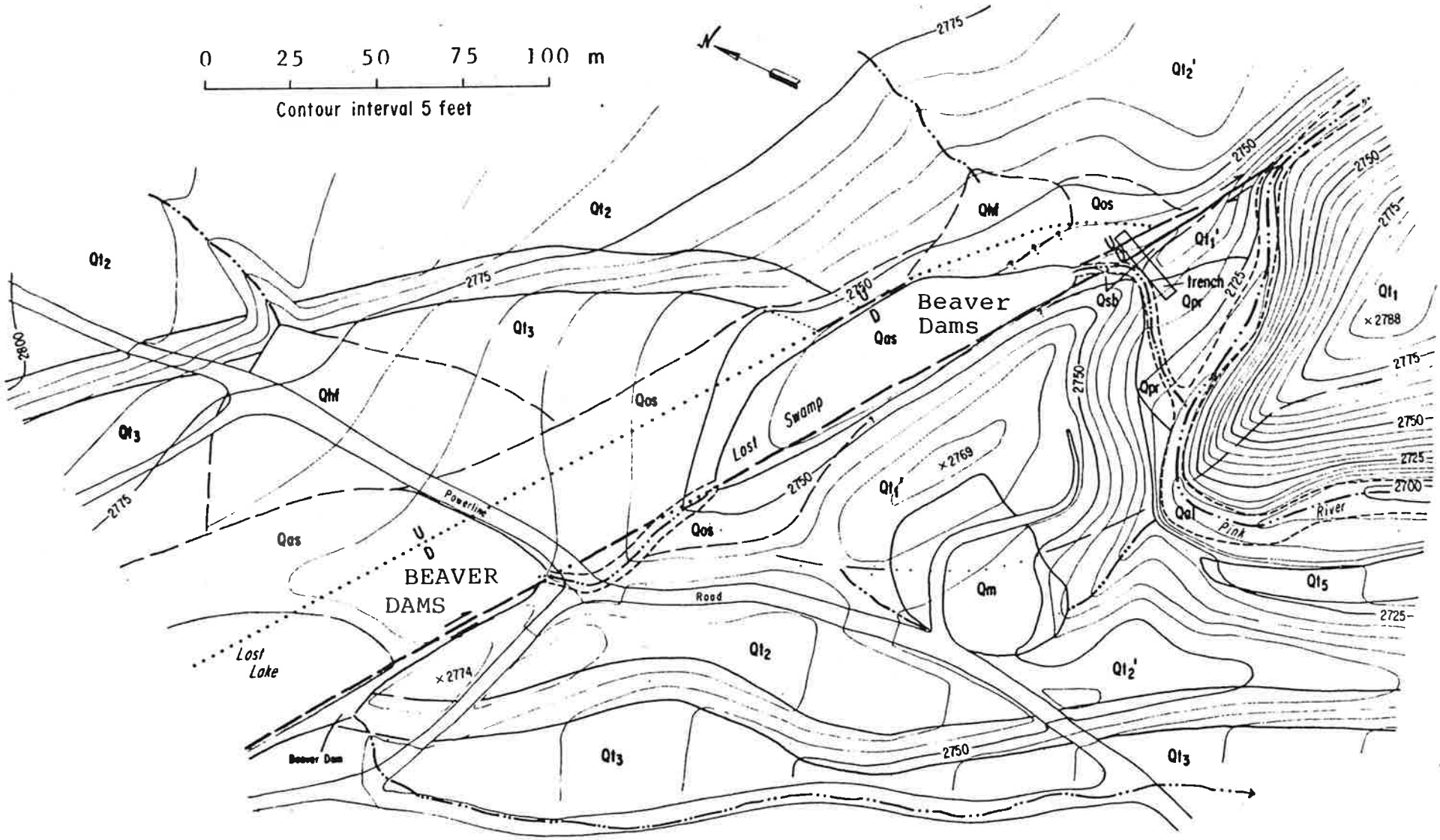

Figure 5. Plane table map of the Lost Swamp area, showing the offset of the riser between Qt-3 and Qt-2 and the excavation site. The Qhf deposits were laid down by streams from the north that were isolated by the incision of Pink River below Qt-5. While Qhf was being deposited, the depression overflowed down the gully buried by the power-line tower fill (Qm); this gully is graded to the Qt-5 level in Pink River. Hill 2769 is too high to be a portion of Qt-2 and is an eroded remnant of Qt-1, around which the Lost Swamp depression drained until the abandonment of Qt-5. Lost Lake drains either into Lost Swamp or down Qt-3, depending on the relative heights of the beaver dams at the 2 sites.

EXPLANATION FOR FIGURE 5

Contact, geologic and geomorphic, solid where certain, dashed where inferred, and dotted where buried.

Current alluvial contact.

Minor stream; active or abandoned channel.

Fault, with arrows and symbols indicating sense of motion; solid where certain, dashed where inferred, and dotted where buried.

UNITS

Qal	Present-day alluvium.
Qas	Modern swamp deposits; peat or lake clay, depending on the depth of water.
Qm	Man-made fill (here, a powerline tower pad).
Qos	Old swamp deposits (where distinguished); peat or lake clay deposited in Lost Swamp before Pink River captured the area.
Qhf	Holocene fanglomerate; dominantly pink sand deposited from the north before Pink River captured the drainage and cut off flow across the terraces.
Qt_5	Terrace of Pink River, cut into Qoa-c gravels deposited by Lone Pine Creek.
Qt_{4-2}	Terraces cut by Lone Pine Creek into Qoa-c gravel.
Qt_1	Fill terrace surface on Qoa-c gravel.
Qt'_{2-1}	Eroded remnant of a higher terrace; no longer associated with a geomorphic surface but high enough that it is clearly not a younger terrace.

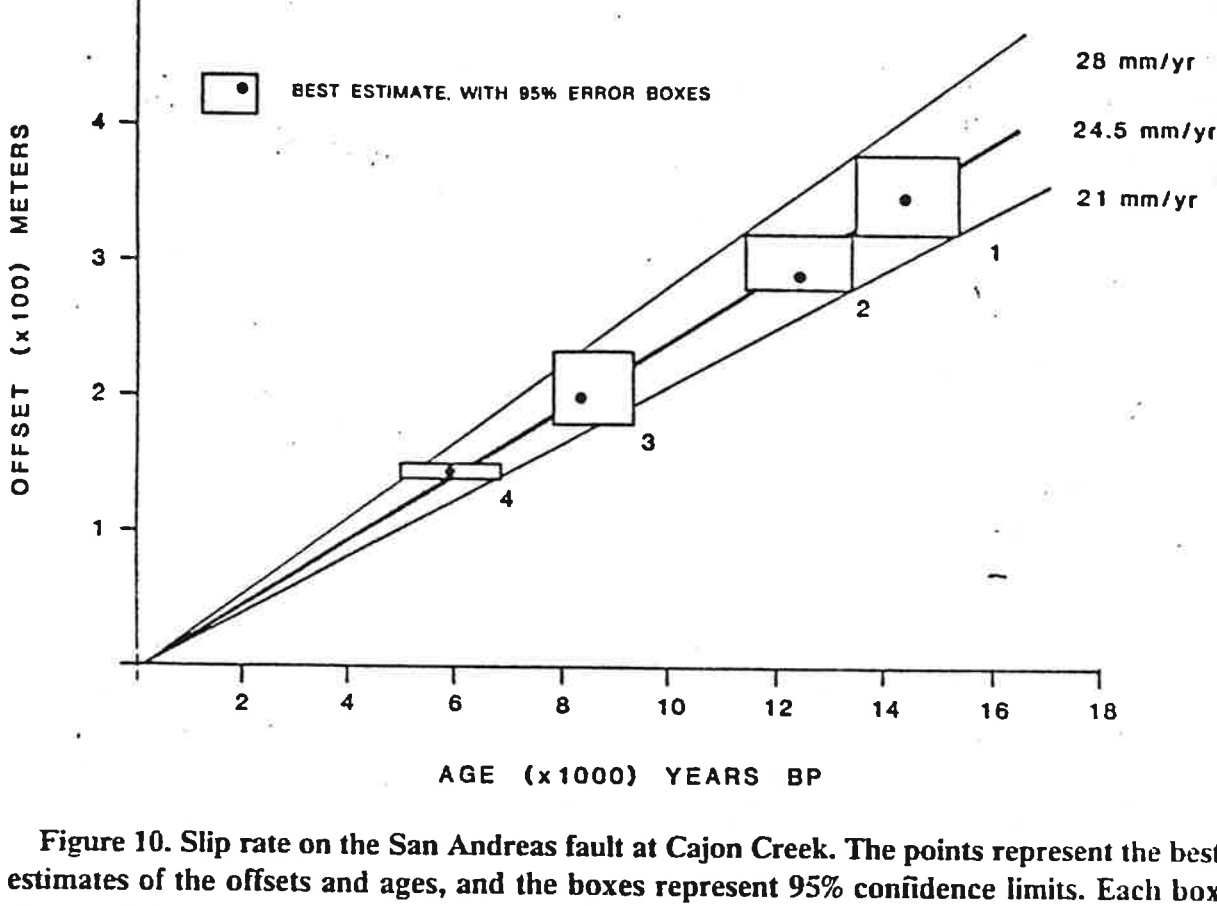

Figure 10. Slip rate on the San Andreas fault at Cajon Creek. The points represent the best estimates of the offsets and ages, and the boxes represent 95% confidence limits. Each box represents independent offset features, radiocarbon dates, and geologic assumptions. The points are not in the center of the boxes due to the asymmetric limits on some of the ages and measurements. The heavy line represents the best estimate of the slip rate at Cajon Creek, and the lighter lines are the limits on the rate, constrained to touch each box. The starting point for each line is 180 yr ago, the best estimate for one-half recurrence interval after the last earthquake (see text for details).

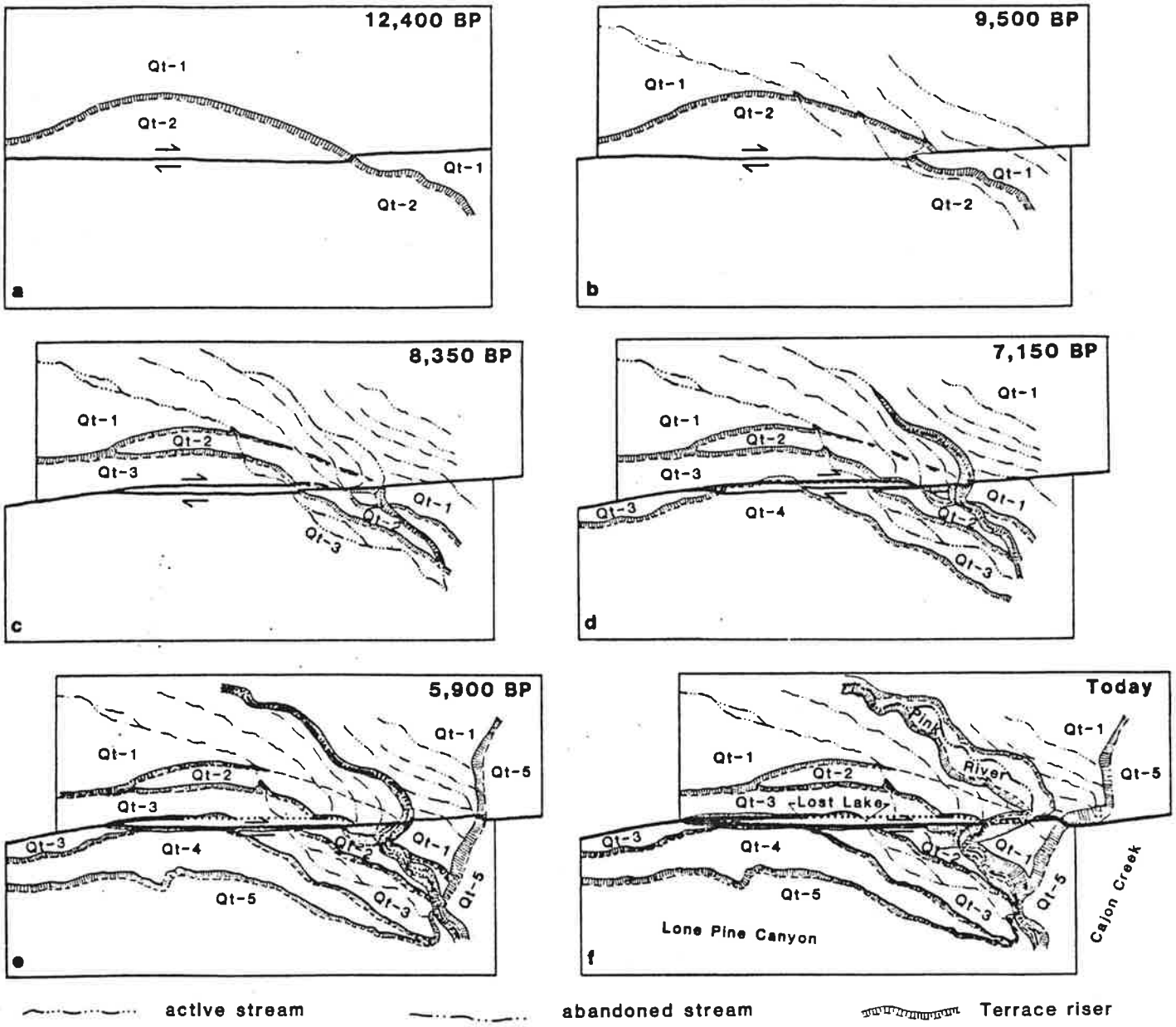

Figure 7. Schematic development of the Lost Lake area. The area shown is the central 2/3 of Figure 4. The reconstruction demonstrates the progressive offset and erosion of the terraces and the development of the Lost Lake depression. Before the drainage from the north was consolidated into Pink River, considerable erosion obscured the older terraces' location. Since the consolidation, the terraces have remained unchanged.

A complicated zone of faulting wraps around the southwest edge of the San Bernardino Mountains north of the North Branch (Fig. 2). Most of these faults are inactive, and those that are active produce only minor displacements of Qoa-d. Like the North Branch, the active faults are predominantly normal and cannot be accommodating a significant fraction of the total slip of the San Andreas system. A fault mapped south of the San Andreas is also dip slip and offsets Qoa-d ~10 m (Fig. 2). The San Andreas fault is the only fault that has accumulated significant lateral offset since the deposition of Qoa-d. The rates determined in this study therefore are inferred to be representative of the fault southeast of its junction with the San Jacinto fault.

The similarity of the offsets of features that are mapped directly to the fault zone with those that are extrapolated from up to several hundred metres away argues against significant distributed shear extending beyond a few metres of the mapped faults. The trench excavated into Lost Swamp and several other exposures of the San Andreas reveal undisturbed Qoa-c gravels within a metre of the edge of the fault zone (for example, Fig. 12). These observations suggest that the fault is accumulating slip across a very narrow zone and that distributed shear is not a significant problem, so the slip rate can be determined from the offset of very minor features.

Faulting near Lost Swamp and Lost Lake

The depression occupied by Lost Lake and Lost Swamp contains critical data for several of the slip-rate values and for the tentative recurrence interval for earthquakes on the San Andreas fault. For this reason, a detailed description of its setting is included. A key point in understanding the history of the depression and in matching the terraces across the fault zone is

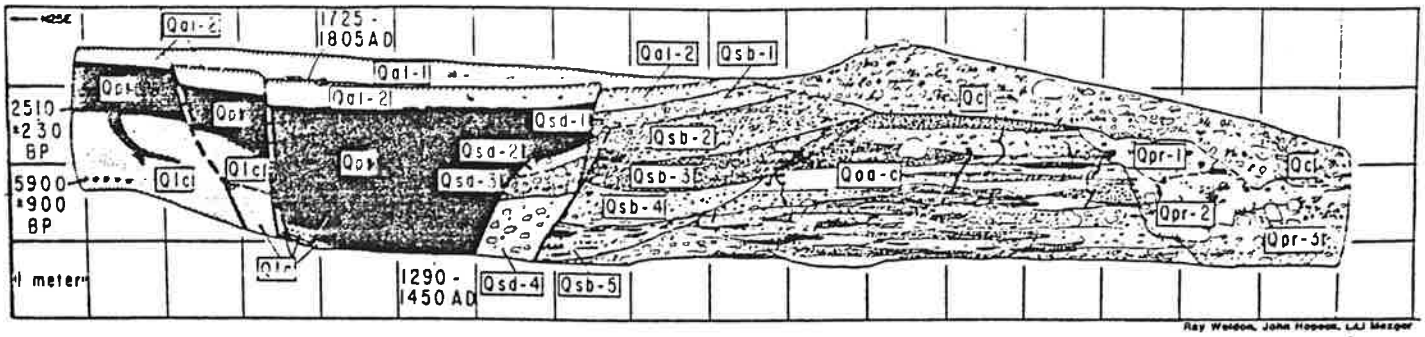

Figure 12. Trench log of the excavation at the southeast end of Lost Swamp. The geomorphically evident main trace occurs 7 m from the northeast end of the excavation. The faults at the northeast end of the excavation appear to be predominantly dip slip. No faulting is observed southwest of the main trace of the fault. The buried ground surface (with the wood on it) between Qal-1 and Qal-2 represents the surface before the last earthquake. The wedge-shaped units between Qoa-c and the fault are breccias shed off paleoscarps that have been buried and eroded (see Fig. 14).

EXPLANATION FOR FIGURE 12

Fault: solid where certain and dashed where uncertain.

Major depositional contact: solid where certain and dashed where approximate.

Minor depositional contact within a major unit: solid where certain and dashed where approximate.

Ground surface: active or buried O-horizon.

Ground squirrel burrows.

Rocks: most clasts larger than ~5 cm were mapped on the log in the field.

Major fissure.

Manganese oxide stains.

Calcareous coating or laminations.

UNITS

Qc	Colluvium being shed into Pink River and the creek that drains Lost Swamp (up which the excavation was cut).
Qal-1	Recent fine-grained alluvium and colluvium shed into Lost Swamp from the east; sole unfaulted unit in the swamp; capped by an O-horizon.
Qal-2	Similar to Qal-1 but faulted and separated from Qal-1 by a buried O-horizon; Qal-2 becomes coarser to the southwest and probably contains some debris off the scarp.
Qsb-1	Transitional between Qal and Qsb-2-5; has coarse debris off the scarp and some fine-grained debris from the east.
Qsb-2-5	Scarp breccia; reworked material derived from Qoa-c off the scarp.
Qsd-1	Like Qsb units but completely within the fault zone.
Qsd-2-4	Scarp deposits completely within the fault zone and containing peaty or clayey matricies; probably breccia shed into the swamp.
Qp	Massive, poorly sorted organic-rich sandy clay; referred to as the "peaty unit" in the text.
Qlc	Relatively organic-free lake clay; contains heterogeneously distributed sand, silt, gastropod shells, and rare pebbles.
Qpr-1 Qpr-2 Qpr-3	Channel fill of Pink River; generally pink, conglomeratic, moderately well-sorted sand that is locally cemented by $CaCO_3$.
Qoa-c	Late Pleistocene river gravels and sand deposited by Lone Pine Creek; the size and sorting of individual units is illustrated by the size, spacing, and regularity of the pebbles and sand grains.

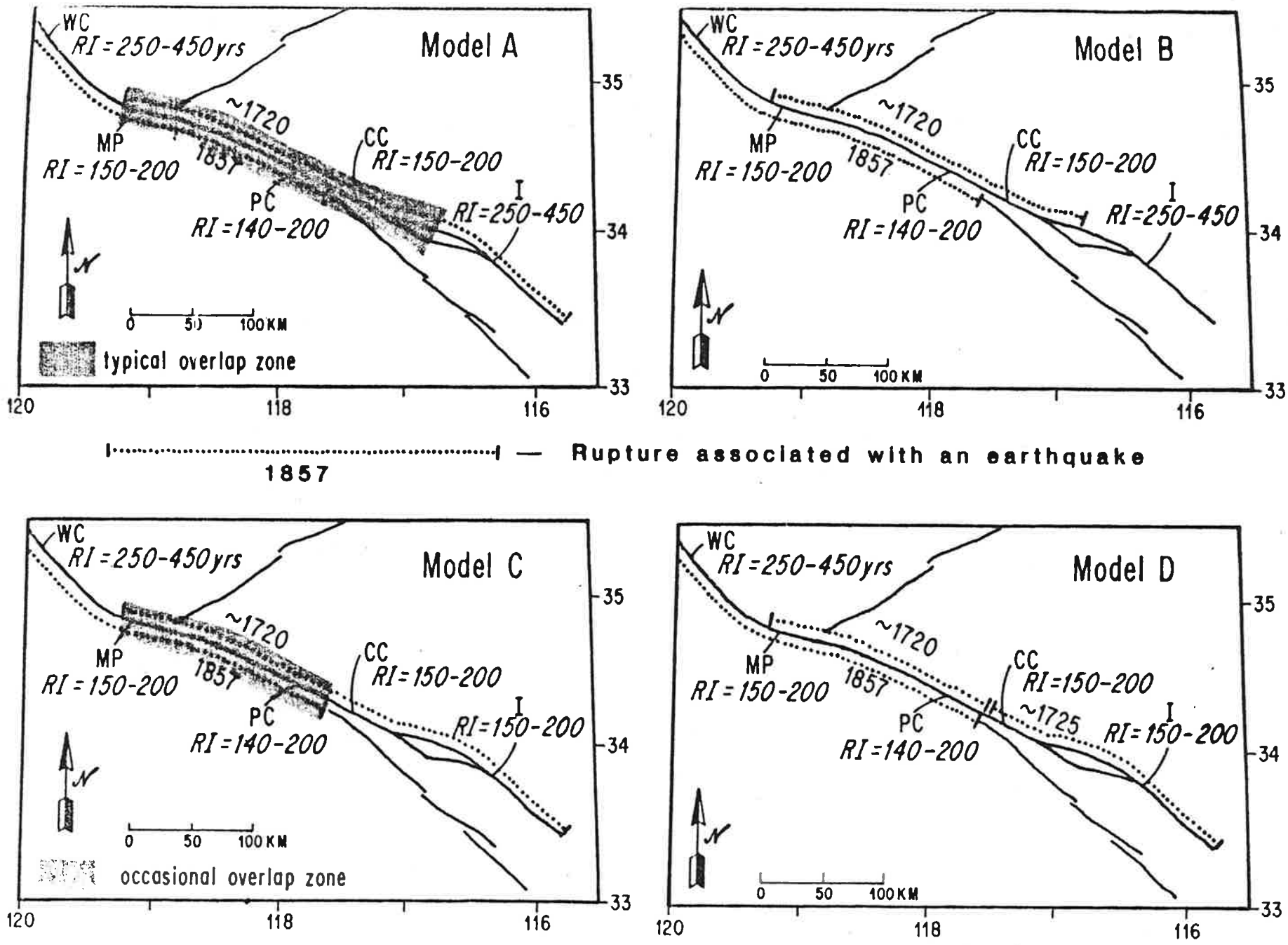

Figure 15. Models for the distribution of rupture associated with recent earthquakes to account for the recurrence intervals observed for the southern San Andreas fault. In models A and B, the recurrence interval (RI) for the southern big bend region (near I) is assumed to be the same as that north of the northern big bend (WC). In models C and D, the recurrence interval for the southern big bend region is the same as the record at Cajon Creek. In models A and C, all events are inferred to be centered at the bends in the fault. In models B and D, there are also events that only rupture the straight stretch between the bends. All of the models suggest that the most likely earthquake on the southern San Andreas would be one centered at the southern big bend. The timing and extent of rupture of the expected event varies with the model (see text).

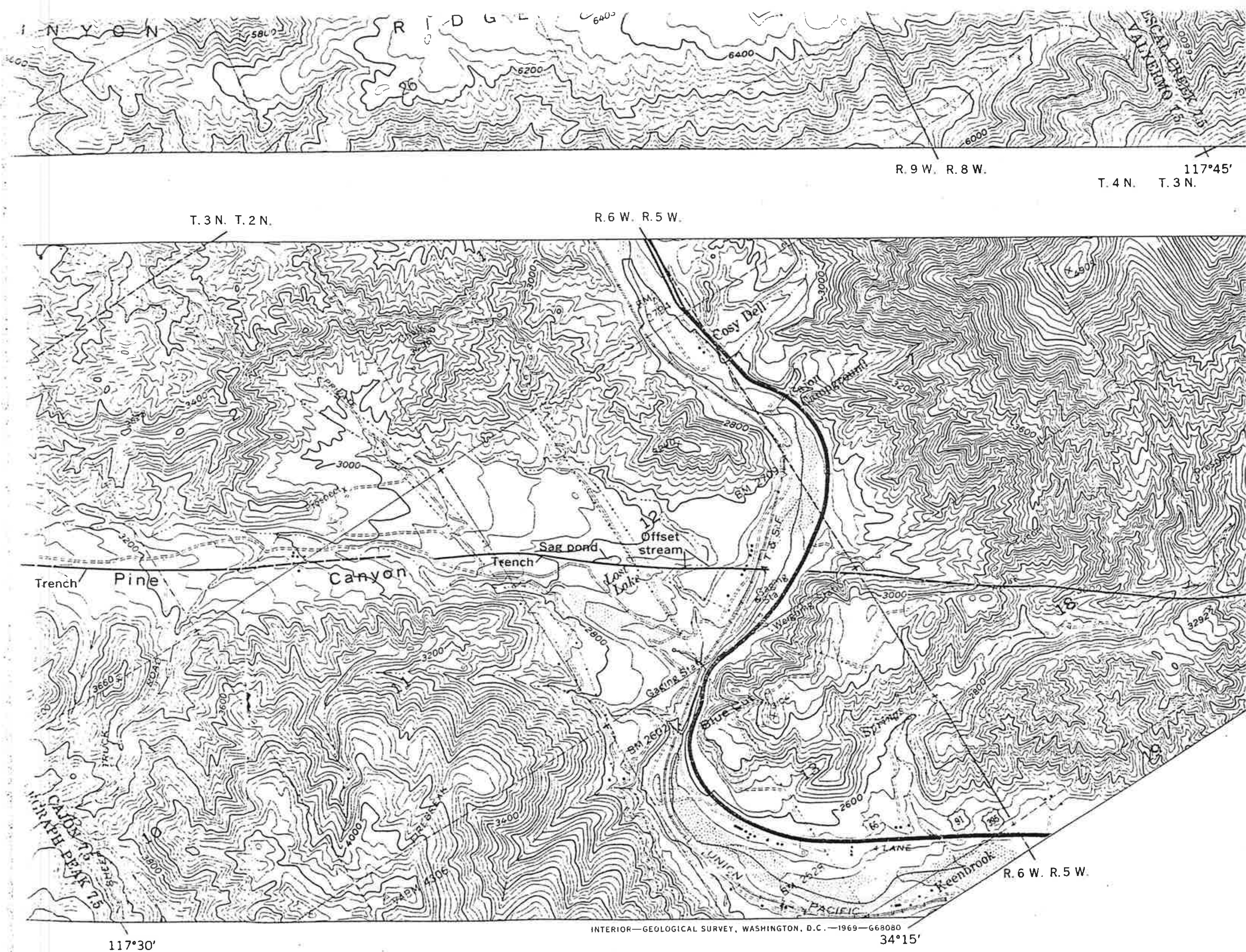

R I D G E
VALYERMO 7.5
R. 9 W. R. 8 W.
117°45'
T. 4 N. T. 3 N.
T. 3 N. T. 2 N.
R. 6 W. R. 5 W.
Cosy Dell
Campground
BM 2709
Offset stream
Sag pond
Trench
Pine
Canyon
Lost Lake
T. & S.F.
Gaging Sta
Blue Cut
Springs
BM 2602
Keenbrook
UNION PACIFIC
BM 2625
LANE
R. 6 W. R. 5 W.
CAJON 7.5
117°30'
INTERIOR—GEOLOGICAL SURVEY, WASHINGTON, D.C.—1969—G68080
34°15'

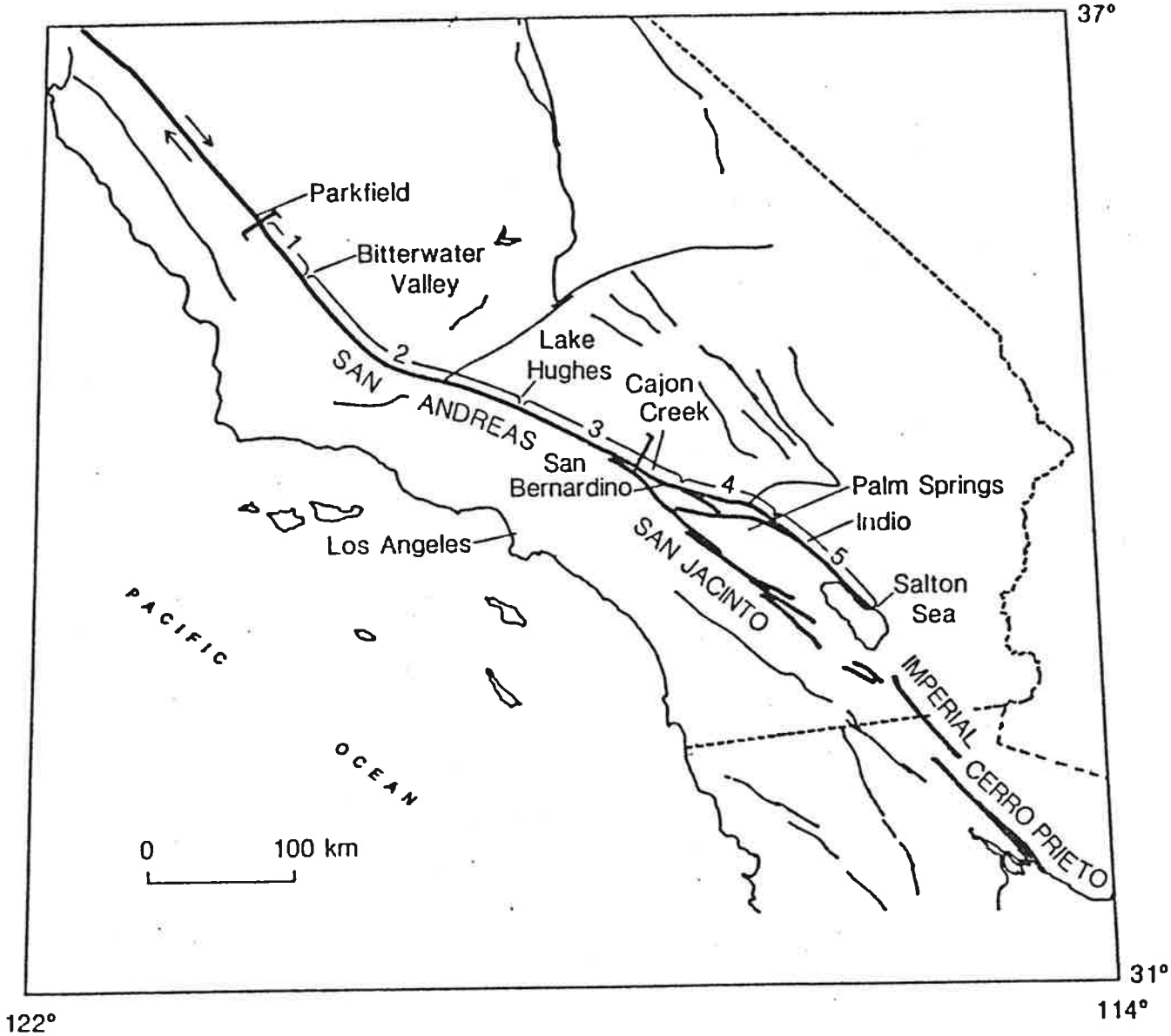

Fig. 1. Map of southern California showing San Andreas, Imperial, Cerro Prieto, and San Jacinto fault traces. Numbered brackets identify sections of brittle fault patch. Large square brackets enclose approximate rupture length of 1857 earthquake [*Sieh*, 1978].

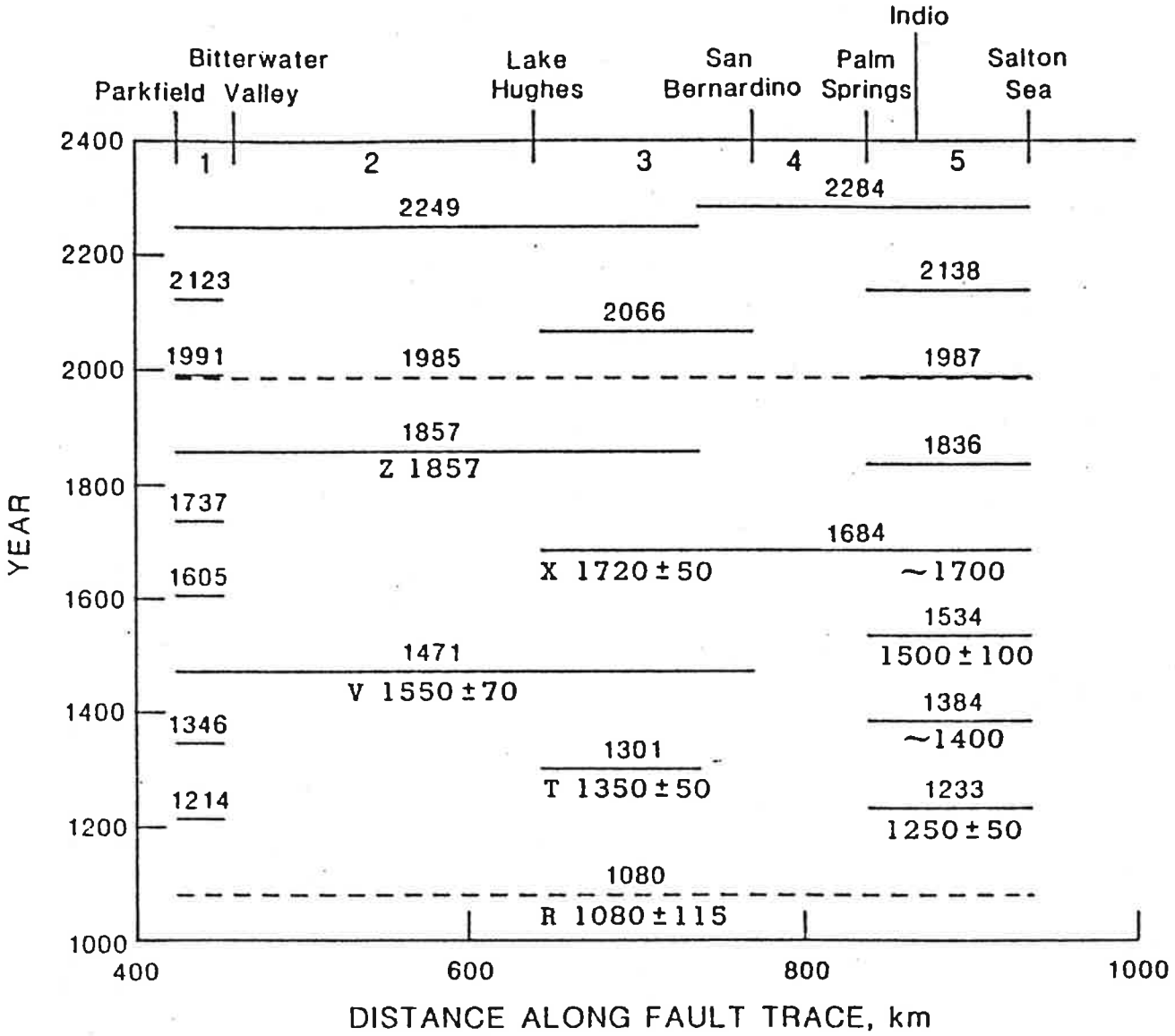

Fig. 5. Space-time diagram showing computed instabilities as solid horizontal lines. Dates of instabilities are above lines. Names and dates of earthquake offsets are below lines. Fault offset data are from *Sieh and Jahns* [1984], *Weldon and Sieh* [1985], and *Sieh* [1984*a*, *b*]. Dashed lines marked 1080 and 1985 are for reference and are not instabilities. Numbers and vertical ticks at top of figure show locations of patch sections 1–5.